RADIOLOGICAL IMPLICATIONS OF ARTISANAL GOLD MINING ACTIVITIES IN GABABIYU, MINNA METROPOLIS, NIGERIA

BY

GOMINA, Mahmoud

MTech/SPS/2017/6948

DEPARTMENT OF PHYSICS

FEDERAL UNIVERSITY OF TECHNOLOGY

MINNA

SEPTEMBER, 2021

RADIOLOGICAL IMPLICATIONS OF ARTISANAL GOLD MINING ACTIVITIES IN GABABIYU, MINNA METROPOLIS, NIGERIA

BY

GOMINA, Mahmoud

MTech/SPS/2017/6948

A THESIS SUBMITTED TO THE POSTGRADUATE SCHOOL FEDERAL UNIVERSITY OF TECHNOLOGY, MINNA, NIGERIA IN PARTIAL FULFILMENT OF THE REQUIREMENTS FOR AWARD OF THE DEGREE OF MASTER OF TECHNOLOGY (MTech) IN APPLIED NUCLEAR PHYSICS

SEPTEMBER, 2021

ABSTRACT

Radiological contaminations of the human environment due to anthropogenic activities have been associated with significant human health challenges. Forty surface soil samples collected at random from Gababiyu artisanal gold mining site in Minna were assessed for their radiological contents using gamma spectrometric technique which employs NaI (Tl) detector. Radiological hazard parameters were also computed from the measured activity concentrations in order to assess the level of exposure of the miners and the public to ionising radiation. Specific activities of ^{226}Ra, ^{232}Th and ^{40}K ranged from 10.27 ± 2.88 to 152.60 ± 3.80 Bq.kg^{-1}, 32.67 ± 1.93 to 185.90 ± 6.06 Bq.kg^{-1} and 35.18 ± 1.45 to 947.50 ± 7.51 Bq.kg^{-1} respectively, with mean values of 65.06 ± 4.20, 87.63 ± 2.89 and 267.94 ± 4.29 Bq.kg^{-1} in sequence. The mean values for ^{226}Ra and ^{232}Th were above the UNSCEAR stipulated global averages. Thus, indicating that the soil bears significant concentrations of ^{226}Ra and ^{232}Th. Computed average absorbed dose rate at 1 m above ground was 94.16 nGy.h^{-1} with corresponding mean annual dose equivalent of 0.22 mSv.y^{-1} and average excess lifetime cancer risk of 0.76×10^{-3}. These values were all below respective safety limits set by UNSCEAR. The results of this investigation therefore indicated minimal radiological risk associated with artisanal gold mining activities in the studied area.

TABLE OF CONTENTS

CHAPTER THREE

CHAPTER FOUR

LIST OF TABLES

LIST OF FIGURES

LIST OF PLATES

LIST OF ABBREVIATIONS

AEDE: Annual Effective Dose Equivalent

AGDE: Annual Gonadal Dose Equivalent

AGI: American Geosciences Institute

AUI: Activity Utilisation Index

CERT: Centre for Energy Research and Training

CPS: Counts Per Second

ELCR: Excess Lifetime Cancer Risk

IAEA: International Atomic Energy Agency

ICRP: International Commission on Radiological Protection

LGA: Local Government Area

MCA: Multi-Channel Analyser

NNRA: Nigerian Nuclear Regulatory Authority

NORM: Naturally Occurring Radioactive Materials

NYSDH: New York State Department of Health

PHTE: Potentially Hazardous Trace Elements

PMT: Photo-Multiplier Tube

UNEP: United Nations Environment Programme

UNSCEAR: United Nations Scientific Committee on the Effects of Atomic Radiation

USNRC: United States Nuclear Regulatory Commission

WNA: World Nuclear Association

CHAPTER ONE

1.0 INTRODUCTION

1.1 Background of the Study

For survival and development, mankind requires natural resources which are randomly distributed on earth (Candeias *et al.*, 2018). Mining and mineral extraction occurs wherever natural resources (metallic, non-metallic minerals and fossils) are present and economically viable (Ako *et al*., 2014). One of the most precious and economically viable natural resource that has continuously attracted the attention of miners is gold. On a large scale, gold-mining yields foreign exchange and economic development. However, Several gold-rich rural areas in Nigeria have been dominated by artisanal miners who are ill-equipped, uneducated and have little appreciation of the environment (Sabo *et al.*, 2018). Artisanal or small-scale mining circumscribes informal, small, medium, legal and illegal mining activities involving the use of unsophisticated tools and techniques to extract mineral resources (Sabo *et al.*, 2018). In developing countries (particularly in West Africa), the environmental consequence of artisanal gold mining has been assessed and well documented (Hilson, 2002; Lacerda and Salomons, 1998; Meech *et al*., 1998; Hollaway, 1993 and Mireku-Gyimah and Suglo, 1993). Mining processes incite depletion of the environment such as land degradation, de-vegetation, air and water pollutions and loss of aquatic organisms (Ako *et al*., 2014).

Nigeria is a gold-rich country. Gold deposits are found in Northern Nigeria and Iperindo, Osun State (Okere, 2018). Nigeria has gold deposits averaging 21370 kg from 2000 to 2018. This number attained an all-time high of 21400 kg in the first quarter of 2018 (Okere,

2018). However, poor attention from the government towards exploiting this mineral, unemployment and extreme poverty have driven large number of people into the local mining occupation. These occupational artisanal miners are from socially and economically marginalised communities (Pure Earth, 2008). They are also uninformed of the implications of mining activities to the environment and human health.

United Nations Scientific Committee on the Effects of Atomic Radiation (UNSCEAR) (2000) identified mining as a potential cause of exposure to naturally occurring radioactive materials (NORM) (Faanu *et al*., 2016). Mining activities propagate NORM and other Potentially Hazardous Trace Elements (PHTE) within the human environment. Wherever these NORM and PHTE are present at levels above the prescribed safety limits by UNSCEAR (2000), they become detrimental to humans and the environment in general. Exposure to the ionising radiation emitted by NORM pose radiological risk to humans and the environment (Alharbi, 2016). The probability and nature of effects induced in humans depend on the radiation dose received by an individual. Such effects may be somatic, occurring only in the exposed individual or genetic, occurring in the descendants of the exposed individual (New York State Department of Health (NYSDH), 2007).

For decades, Gababiyu area in Minna Metropolis has been known for artisanal gold mining activities. Most recently, the area have been marked as proposed site for El-Amin University. Consequently, the population of the proposed University will occupy a degraded environment. Furthermore, there is a likelihood of NORM and PHTE propagation within the mining environment. It has therefore become necessary that the radiation load on the miners and the public as a result of this anthropogenic activity be evaluated to check the level of radiation exposure.

In Nigeria, there is a general lack of information regarding concentration of NORM and associated radiological parameters from local mining areas. Thus, this work seeks to assess the radiological implications of artisanal mining in Gababiyu artisanal gold mine in Minna Metropolis, Nigeria.

1.2 Statement of the Research Problem

Associated with mining and mineral processing are potential adverse health risks that are more significant to occupationally exposed individuals. Artisanal mining is associated with the generation of significant mining wastes (tailings) which are indiscriminately disposed off in the surrounding environment. Additionally, natural processes like rainfall and leaching processes wash NORM to river bodies, thereby radiologically contaminating the water bodies. The tailings are also used as aggregates of building materials, which thus enhances radiation concentration in human dwellings. The human food chain is also contaminated as crops cultivated around the study area absorb NORM from the soil. More artisanal mines have been surveyed in Ghana and Nigeria due to their huge gold deposits. Poverty has also driven more rural dweller into the mining occupation in these two countries. Furthermore, artisanal miners ignore necessary safety procedures while mining for gold as they are unaware of the radiological implications of exposure to NORM. All these processes potentially increase human exposure to radiations, some to levels that seem detrimental to human health as well as the environment. Thus, this work is aimed at determining the level of exposure of miners and the environment to NORM.

1.3 Aim and Objectives of the Study

This study is aimed at quantifying the radiation dose to miners and the environment from artisanal mining activities around Gababiyu pre-industrial goldmine, in Minna Metropolis through gamma spectrometry.

The objectives are to:

   i.   determine the specific activity concentration of naturally occurring radionuclides (^{226}Ra, ^{232}Th and ^{40}K) in soil around Gababiyu pre-industrial gold mining site, Minna.

  ii.   compute radiological parameters and assess the radiological health risk related to mining in the area.

1.4 Scope of the Study

The cynosure of this research is to assess the radiological health risk associated with small-scale gold mining in Gababiyu, Minna Metropolis. Through the determination of the activity concentration of naturally occurring radionuclides in 40 soil samples collected from Gababiyu artisanal gold mine. Using identification and quantification of radionuclides by examining the gamma-ray energy spectrum produced in a Sodium Iodide Thalium-activated (NaI[Tl]) gamma-ray spectrometer in the department of radiation biophysics of the Centre for Energy Research and Training (CERT), Zaria.

Natural radionuclides detection in this study is limited to gamma energy peaks (channels) of 1460.0, 2614.5 and 1764.0 KeV analysing for ^{40}K, ^{232}Th and ^{226}Ra respectively. They exhibit photon intensity sufficient for gamma-ray spectrometry and contribute significantly to the doses dispersed in the environment and received by human populace. From the

determined activity concentration, radiological parameters are computed and compared with globally recommended thresholds for occupational exposure to radiation. Determined values above the stipulated threshold will indicate significant radiological contamination and associated health risks while values below the threshold will indicate minimal radiological risks.

1.5 Significance of the Study

Understanding the behaviour of radionuclides in the environment provides information of related parameter values for radiological assessments. These assessments are relevant for monitoring environmental radioactivity levels and remediation.

It is essential to determine the activity concentration of NORM in Gababiyu pre-industrial gold mine as the area under study and its immediate environs may be at risk of exposure to radiation dose(s) resulting from the artisanal gold mining activities. Upon comparison with global screening level for occupational radiation exposure, the estimated dose rate from this study will establish the radiological safety for artisanal mining in the region. The outcome of this study will enlighten the miners who are occupationally exposed to NORM on the need for radiological protection during their routine mining processes. Results of this research will serve as baseline data for the region upon which future determination can be compared with. The baseline data will be relevant for evaluating potential radiological health risk to the populace of the proposed El-Amin University. Also, there are no defined guidelines by the Nigerian Nuclear Regulatory body for existing mining areas in Nigeria. Therefore, there is need for radioactivity measurements in artisanal gold mining communities in Nigeria to establish baseline data for safety and future comparison. This will enable the assessment of the variations of NORM concentration due to mining and

evaluation of contamination levels. Also, government environmental and health regulatory agencies will find the result of this study valuable for policy making as regards to safeguarding environmental and human health. This is achievable by expanding future determinations to other gold mining communities and immediate environs.

CHAPTER TWO

2.0   LITERATURE REVIEW

Radioactive nuclides transform to stable ones (to attain stability) and in the process dissipate mass-energy. This phenomenon termed radioactivity and related concepts are discussed in this section. Radioactivity has played a very important role in the advancement of nuclear physics as it has been essential in understanding the nature of the atomic nucleus. Environmental assessment of radiation levels is achieved through the knowledge of radiations and their interaction with matter. The basic concepts of radioactivity are reviewed in this section. Also reviewed are similar work done by other authors in this field of research.

2.1 Radioactivity

Discovered by Henri Becquerel in 1896, radioactivity is also termed nuclear transformation or disintegration and radioactive or nuclear decay. It is the phenomenon in which the nuclei of elements emits radiation in the form of energised particles or electromagnetic radiation (γ ray photons) or both (Khan, 2003). An unstable parent nucleus releases energy (particle or electromagnetic radiation) during decay and transforms into a lighter daughter nucleus which may be stable or unstable (Bailey *et al.*, 2014). The unstable daughter further disintegrate in a sequence up to a stable nuclear configuration (Bailey *et al.*, 2014). Nuclides that are unstable and achieve greater stability through radioactive decay are termed radionuclides (Alpen, 1998).

Quantities and units are used in describing and quantifying the measure of radiation. Table 2.1 is a summary of some SI derived quantities associated with radioactivity. Their

preferred symbol, unit, dimension, and older unit usage/conversion are also described in sequence.

Table 2.1: SI derived quantities and units of radioactivity

Quantity	Symbol	Unit	Dimension	Use/Conversion of older units
Activity	A	Becquerel (Bq)	s^{-1}	Radioactivity of objects
Specific activity	A	Becquerel per kilogram (Bq/kg)	$kg^{-1}\,s^{-1}$	Radioactivity of unit mass
Surface activity	a_s	Becquerel per metre squared (Bq/m^2)	$m^{-2}\,s^{-1}$	Radioactivity of unit area
Exposure	X	Coulomb per kilogram (C/kg)	$kg^{-1}sA$	Ionizing effect of X and gamma rays in air
Exposure rate	$\dot{X}$	Ampere per kilogram (A/kg)	$A\,kg^{-1}$	Exposure per unit time, gamma radiation field $1\mu R/h = 7.17 \times 10^{-14}\,A\,kg^{-1}$
Dose	D	Gray (Gy)	$m^2\,s^{-2}$	Absorbed dose 1 rad$=10^{-2}$ Gy 1R$=8.69 \times 10^{-3}$ Gy (in air)
Dose rate	$\dot{D}$	Gray per second (Gy/s)	$m^2\,s^{-3}$	Gamma radiation field $1\mu R/h = 8.69$ nGy/h in air
Dose equivalent	H	Sievert (Sv)	$m^2\,s^{-2}$	Biological effects of radiation 1 rem$=10^{-2}$ Sv
Photon equivalent dose rate	$\dot{H}_x$	Sievert per second (Sv/s)	$m^2\,s^{-3}$	Dose equivalent per unit time
Equivalent dose	H_T	Sievert (Sv)	$m^2\,s^{-2}$	Biological effects of radiation
Effective dose	E	Sievert (Sv)	$m^2\,s^{-2}$	Biological effects of radiation to man

Source: IAEA (2003)

2.1.1 Natural sources of radiation

Human radiation exposure is inevitable. Most of the world's population exposures to radiation are due to natural sources (UNEP, 2016). Since creation, earth's environment has been exposed to radiations from outer space and those from radioactive materials present in its crust and core (UNEP, 2016). The global mean effective dose to an individual is about 2.4 mSv and varies from about 1 to more than 10 mSv depending on the location where people live (UNEP, 2016).

Natural radiation emanates from cosmic, terrestrial and internal radiation sources. Cosmic radiations are natural background radiations originating from outer space. They are composed of penetrating ionizing radiation reaching the earth like a steady drizzle of rain sent by the sun and stars. The amount (dose) of cosmic radiation received from outer space is influenced by the unevenness in elevation, conditions of the atmosphere, and Earth's varying magnetic field (USNRC, 2017). Terrestrial radiation is the fragment of the natural background radiation released on earth by naturally occurring radioactive materials such as uranium, radium and thorium (USNRC, 2017). These materials are compositions of soil, water and vegetation. Essentially, all air contains radon, water contains small amount of uranium and thorium, and all organic matter contains radioactive carbon and potassium. From birth, every individual exhibit internal radiation, resulting mainly from radioactive potassium-40 and carbon-14 inside the human body. Thus, they are sources of exposures to others (USNRC, 2017). Some of these contaminants are consumed with food and water while others are inhaled (such as radon). Although the sources are not artificial, exposure can be modified by man-made choices, such as where and how people live or what they eat and drink.

2.1.2 Types of nuclear decay

Becquerel's experiments on the fluorescence of uranium salts revealed that a photographic plate enveloped in black paper was affected by the salts kept outside the paper (Kakani and Kakani, 2008). The observed effect indicates that uranium emits radiations that are independent of any external influence. Rutherford classified radioactive emissions as α-and β-rays from his experiments on the penetrating powers of radiation while a third-type, named γ-rays was added by Villard (Kakani and Kakani, 2008). These three emissions constitute the basis of the nuclear decay types which are alpha, beta and gamma decays.

2.1.2.1 Alpha decay

Alpha decay (or α-decay) is defined by the ejection of α-particle from a parent nucleus ($^{A}_{Z}X$). The α-particles are nuclei of the helium atoms ($^{4}_{2}He$) and after emission a new nucleus ($^{A-4}_{Z-2}Y$) is formed (Kakani and Kakani, 2008). The radioactive transformation equation for this decay mode is expressed in equation 2.1, α emissions reduces the mass number of the parent nucleus by 4 units and the atomic number by 2 units. However, the mass number and total charge are conserved during transformation.

$$^{A}_{Z}X \rightarrow \,^{4}_{2}He + \,^{A-4}_{Z-2}Y \tag{2.1}$$

Examples of α-decay are expressed in equations 2.2, 2.3 and 2.4:

$$^{238}_{92}U \rightarrow \,^{4}_{2}He + \,^{234}_{90}Th + Q_{\propto} \tag{2.2}$$

$$^{222}_{86}Rn \rightarrow \,^{4}_{2}He + \,^{218}_{84}Po + Q_{\propto} \tag{2.3}$$

$$^{218}_{84}Po \rightarrow \,^{4}_{2}He + \,^{214}_{82}Pb + Q_{\propto} \tag{2.4}$$

Any group of α-particles emitted from the same type of nuclei possesses a definite velocity and energy. They can induce intense ionization in air and can be immobilised by a thin sheet of paper with velocities ranging between 1.5×10^7 and 2.2×10^7 m/s (Kakani and Kakani, 2008). The definite distance they travel within a material is called the range of α-particles in that material.

2.1.2.2 Beta decay

Beta decay (or β-decay) is characterised by the emission of β-particles which are identical with electrons with a mass $\left(\frac{1}{1836}\right)$ of mass of a proton. β-particles are high energy electrons that are much more penetrating than α-particles (Ghoshal, 2014). During β⁻ decay, a parent nucleus ($^A_Z X$) transforms to a daughter nucleus ($^A_{Z+1}Y$) as represented in equation 2.5.

$$^A_Z X \rightarrow\, ^A_{Z+1}Y\ +\ ^0_{-1}e + \bar{v}_e \tag{2.5}$$

The atomic number Z of the parent nucleus is increased by 1 unit (Z+1) in the daughter nucleus while the mass number A is unvaried (isobaric transition) in this decay mode. β-rays cause much less ionization in air but are about 100 times more penetrating than α-rays (Kakani and Kakani, 2008). Up to 0.99 of light-speed, β-particles are emitted with varying energy between zero and a certain maximum (termed end-point energy).

There are two other β-decay processes distinguished by positron emission and electron capture. In positron emission (β⁺ decay), a proton-rich parent nucleus transforms into a neutron and emits a positron $e+$ and an electronic neutrino (v_e). The proton number of the daughter reduces by a unit ($Z_Y = Z_X - 1$) while the mass number remains constant, just as in the case of electron emission. This decay process is described by Equation 2.6 as follows:

$$_{Z}^{A}\text{X} \rightarrow \ _{z-1}^{A}\text{Y} + e^{+} + \upsilon_{e} \tag{2.6}$$

Decay by electron capture may result when an atomic electron that enters inside the nuclear volume is captured by a proton (Bailey *et al.*, 2014). This initiates a proton-neutron transformation and ejection of an electronic neutrino (Bailey *et al.*, 2014). The generic relationship for the decay due to electron capture is expressed as Equation 2.7:

$$_{Z}^{A}\text{X} + \ _{-1}^{0}e \rightarrow \ _{z-1}^{A}\text{Y} + e^{+} + \upsilon_{e} \tag{2.7}$$

2.1.2.3 Gamma decay

Most nuclear reactions are accompanied by gamma (γ) ray production. γ-rays are very high electromagnetic radiations with very short wavelengths. They are about 100 times more penetrating than β-rays. During γ-decay, a nucleus exhibits a transition from one energy state to another with no fundamental change induced in the decaying nucleus (Kakani and Kakani, 2008). This decay mode can be expressed as:

$$_{Z}^{A}\text{X}^{*} \rightarrow \ _{z}^{A}\text{X} + \gamma \tag{2.8}$$

$$_{38}^{87}\text{Sr}^{*} \rightarrow \ _{38}^{A}\text{X} + \gamma \tag{2.9}$$

The principal modes of radioactive decay, with the form of radiation emitted, generic equation and model for each are described in Figure 2.1.

Decay Type	Radiation Emitted	Generic Equation	Model
Alpha decay	$^{4}_{2}\alpha$	$^{A}_{Z}X \longrightarrow ^{A-4}_{Z-2}X' + ^{4}_{2}\alpha$	Parent → Daughter + Alpha Particle
Beta decay	$^{0}_{-1}\beta$	$^{A}_{Z}X \longrightarrow ^{A}_{Z+1}X' + ^{0}_{-1}\beta$	Parent → Daughter + Beta Particle
Gamma emission	$^{0}_{0}\gamma$	$^{A}_{Z}X^* \xrightarrow{\text{Relaxation}} ^{A}_{Z}X' + ^{0}_{0}\gamma$	Parent (excited nuclear state) → Daughter + Gamma ray

Figure 2.1: Common modes of nuclear decay (Bewick *et al*., 2019)

2.1.3 Decay series of naturally occurring radioactive materials (NORM)

Many elements occurring naturally exist with radioactive isotopes. However, only the non-serial potassium and the serial thorium and uranium have radioisotopes that induce gamma-rays of adequate energy and intensity to be determined by gamma spectroscopy. This is because of their relative abundance in the natural environment (IAEA, 2003).

Occurring as 0.01 % of natural potassium, ^{40}K, a radioactive isotope of potassium disintegrate to ^{40}Ar with the release of gamma rays possessing 1.46 MeV energy (IAEA, 2003). Since ^{40}K occurs as a fixed proportion of potassium in the natural environment, the gamma rays emitted by ^{40}Ar can be used to estimate the total amount of potassium present. "The half-life of ^{40}K is 1.30×10^9 years" (IAEA, 2003).

Uranium occurs naturally as the radioisotopes ^{238}U and ^{235}U, individually starting the decay series that terminates in the stable isotopes ^{206}Pb and ^{207}Pb respectively. "The half-lives of ^{238}U and ^{235}U in years are respectively, 4.46×10^9 and 7.13×10^8" (IAEA, 2003).

Thorium exists naturally as the ^{232}Th radioisotope, resulting in a decay series that discontinue with the formation of the ^{208}Pb stable isotope. The half-life of ^{232}Th is 1.39×10^{10} years (IAEA, 2003). The concentrations of ^{238}U nor ^{232}Th in a sample are estimated from the gamma ray emissions of their radioactive daughter products as neither directly emit gamma rays. Figure 2.2 illustrates the disintegration sequence of NORM and the associated modes of decay.
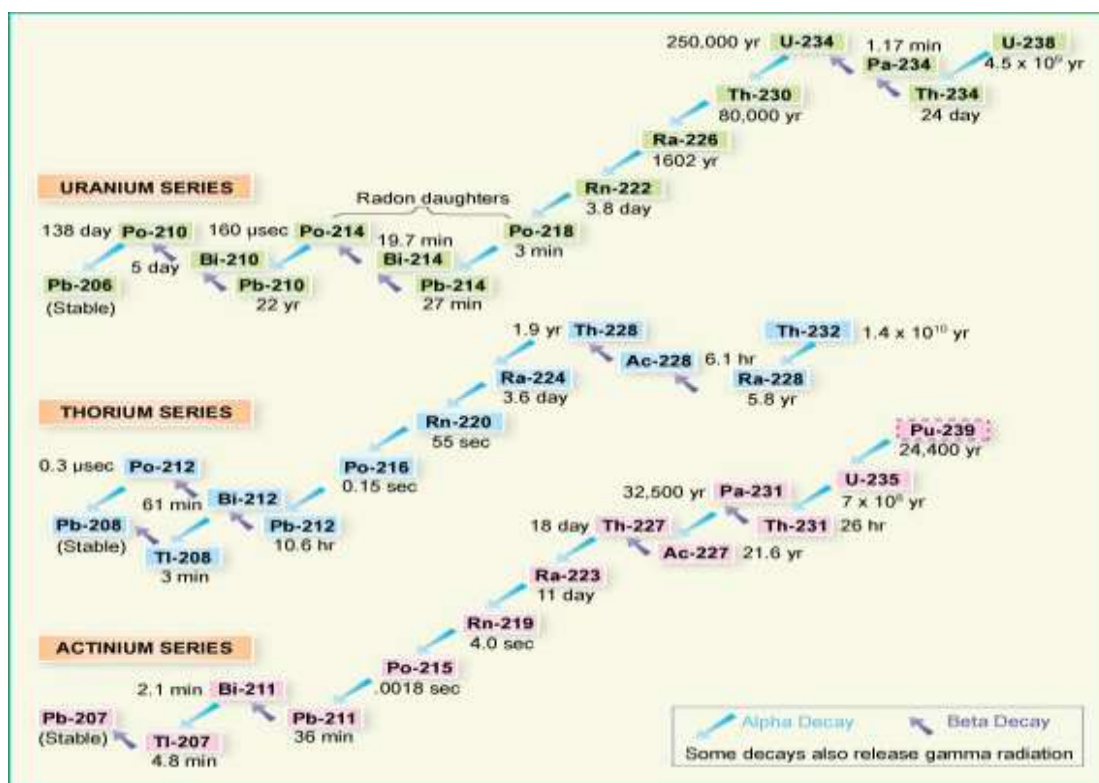
Figure 2.2: Decay series of NORM (WNA, 2014)

The changes observed during α-decay (change in the values A and Z) and β-decay (change in Z value) lead to the formulation of the displacement law. Alpha decay results in the reduction of the mass number (A) of an atom by 4 units and its displacement in the periodic table by two steps to the left. Beta decay leaves the A value of an atom unchanged but shifts the atom's position by one step to the right in the periodic table (Ghoshal, 2014).

These two statements govern the series of decaying naturally occurring radionuclides as illustrated in Figure 2.2. The actinium series is the common name for the uranium-235 series.

2.1.4 Radioactive equilibrium

Radioactive disintegration of the atoms of a parent element, P into a lighter daughter nuclide, D can be symbolically expressed as P→D. The number of atoms of P decreases with time while that of D increases over time. If N number of atoms of P at any instant, then the decay law stipulates that the rate of change of N with time is proportional to N. This is a measure of the activity of P and expressed as:

$$\frac{dN}{dt} \propto N$$

$$\Longrightarrow \frac{dN}{dt} = -\lambda N \tag{2.10}$$

where, λ is the decay constant while the negative sign defines the diminishing of N with increasing time.

Equation 2.1 is solved by integration w.r.t time, t which yields:

$$N(t) = N_o e^{-\lambda t} \tag{2.11}$$

N_o is the number of P atoms present at time, $t = 0$ (before decay).

Equations 2.1 and 2.2 combined can be written in terms of activity as follows:

$$A(t) = \left|\frac{dN}{dt}\right| = \lambda N = \lambda N_o e^{-\lambda t} = A_o e^{-\lambda t} \tag{2.12}$$

The decay law (Equation 2.12) holds for all radionuclides regardless of their decay modes. But the constant of decay (λ) varies. λ is the most important defining characteristic of decaying nuclides (Bailey *et al*., 2014). However, two special time periods called half-life ($T_{1/2}$) and mean (average) life (τ) are used to characterise a particular radioactive substance.

The half-life ($T_{1/2}$) of a radioactive material is the time which the number of nuclei of the material takes to decay to half of its initial value (N_o at $t = 0$). It can also be stated that in the time of one $T_{1/2}$, the activity of the material diminishes to one half of its initial value. Mathemathically:

$$\frac{1}{2}A_o = A_o e^{-\lambda t} \tag{2.13}$$

$$\therefore \frac{1}{2} = e^{-\lambda T_{1/2}} \tag{2.14}$$

Equation 2.14 results to the relationship between λ and $T_{1/2}$ expressed in Equation 2.15:

$$\lambda = \frac{\ln 2}{T_{1/2}} = \frac{0.693}{T_{1/2}} \tag{2.15}$$

The mean life time (τ) of a radionuclide is defined as the time taken for the activity (or number of atoms) to fall to $1/e$ (0.368 or 36.8%) of the initial value (Bailey *et al.* 2014). Therefore, the mean life time is described by the following expression:

$$\frac{1}{e}A_o = A_o e^{-\lambda t} \tag{2.16}$$

$$\Rightarrow e^{-1} = 0.368 = e^{-\lambda \tau} \tag{2.17}$$

by comparing index of e on both ends, Equation 2.17 reduces to a product of the decay constant and the mean life which results to a reciprocal relation between both expressed as Equation 2.18:

$$\tau = \frac{1}{\lambda} \tag{2.18}$$

The relationship between $T_{1/2}$ and τ is obtained by plugging Equation 2.15 in to 2.18 such that:

$$\tau = \frac{1}{\left(\frac{0.693}{T_{1/2}}\right)} = (1.443)T_{1/2} \tag{2.19}$$

A plot of activity for a parent radionuclide, $A_p(t)$ against time, t given in Equation 2.12 is shown in the exponential curve in Figure 2.3 .This represents simple radioactive decay for the initial condition A_p (t=0) = $A_p(0)$. A daughter, D (stable or unstable) is formed from the decay of radioactive parent, P as illustrated. The ideas of half-life ($T_{1/2}$) and the mean life (τ) for the parent nuclide are also illustrated.
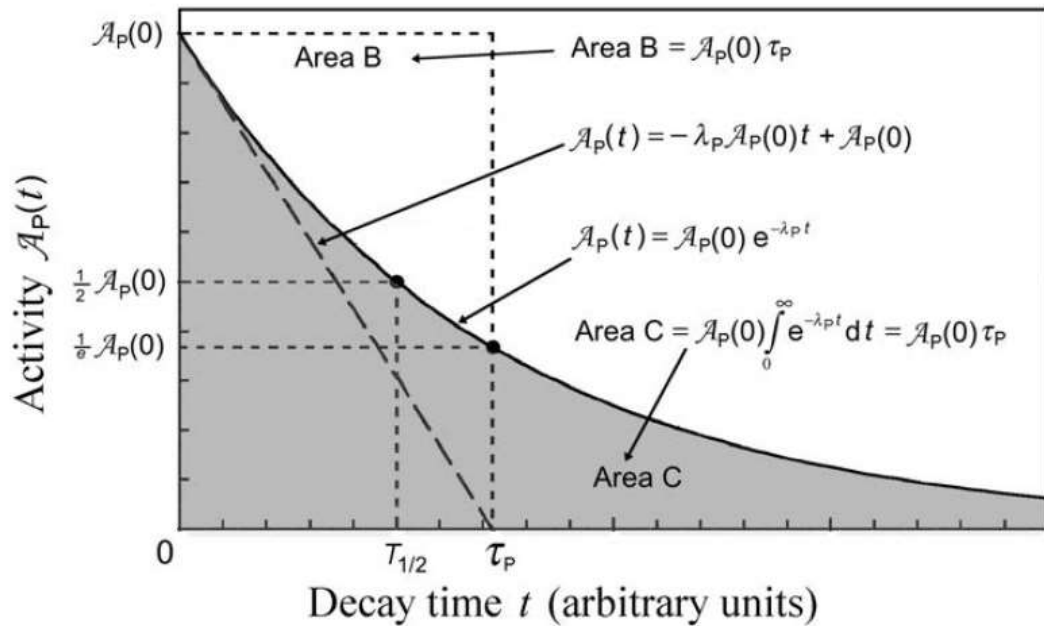
Figure 2.3: Activity of parent radionuclide, $A_p(t)$ against time, t (Bailey *et al.*, 2014)

The region from t=0 to t=∞ (area under the decay curve) is equal to the product $A_P(0)\tau_P$, with $A_P(0)$ being the activity of the parent, P at t=0. The slope of the tangent to the curve at this instant is equal to $\lambda_P A_P(0)$ from the substitution of Equation 2.18 into $A_P(0)/\tau_P$ and this tangent crosses the horizontal axis at τ_P.

During decay modes from P (parent) →D (daughter) → G (grand-daughter) relationships, a certain time, t is attained such that the parent and daughter activities maintain fixed ratio that is constant over time change (Bailey *et al.*, 2014). This condition is called radioactive

equilibrium and it may be transient or secular. The radioactive decay described by Equations 2.11 and 2.12 follows a direct integration into a stable daughter. However, radioactive decay in practical cases consists of two components and are more complicated (Ghoshal, 2014). One is the production of new daughter nuclei, D by the decay of P given as $\lambda_P N_P(t)$ and the second is the loss of D decaying to G given as $- \lambda_D N_D(t)$. Thus, resulting in the expression for $dN_D(t)/dt$:

$$\frac{dN_D(t)}{dt} = \lambda_P N_P(t) - \lambda_D N_D(t) = \lambda_P N_P(0) e^{-\lambda_P t} - \lambda_D N_D(t) \qquad (2.20)$$

Equation 2.20 is resolved by multiplying both ends by an integrating factor of $e^{-\lambda_D t}$ and integrating w.r.t t such that:

$$N_D(t) e^{\lambda_D t} = \frac{\lambda_P}{\lambda_D - \lambda_P} N_P(0) e^{(\lambda_D - \lambda_P)t} + C \qquad (2.21)$$

where, C is the constant integration whose value is determined by subjecting Equation 2.21 to the initial condition that at t=0, $N_D(0)=0$ (no daughter nuclei present).

$$\Rightarrow C = -\frac{\lambda_P}{\lambda_D - \lambda_P} N_P(0) \qquad (2.22)$$

Substituting Equation 2.22 into 2.21 yields the specific solution for 2.20 as follows:

$$N_D(t) = N_p(0) \frac{\lambda_P}{\lambda_D - \lambda_P} \left[e^{-\lambda_P t} - e^{-\lambda_D t} \right] \qquad (2.23)$$

Thus, the activity of the daughter $A_D(t)$ is written as:

$$A_D(t) = N_P(0) \frac{\lambda_D \lambda_P}{\lambda_D - \lambda_P} \left[e^{-\lambda_P t} - e^{-\lambda_D t} \right] = A_P(0) \frac{\lambda_D}{\lambda_D - \lambda_P} \left[e^{-\lambda_P t} - e^{-\lambda_D t} \right] \qquad (2.24)$$

where, $A_D(t) = \lambda_D N_D(t)$ is the activity of the daughter at time t and $A_P(0) = \lambda_P N_P(0)$ is the initial activity of P at zero time unit.

Equilibrium in radioactivity can be explained quantitatively by probing the behaviour of the activity ratio $A_D(t)/A_P(t)$ derived from Equation 2.24 by substituting $A_P(0) = A_P(t) e^{\lambda_P t}$:

$$\frac{A_D(t)}{A_P(t)} = \frac{\lambda_D}{\lambda_D - \lambda_P} \left[1 - e^{-(\lambda_D - \lambda_P)t} \right] = \frac{1}{1 - \frac{\lambda_P}{\lambda_D}} \left[1 - e^{-(\lambda_D - \lambda_P)t} \right] \qquad (2.25)$$

Three scenarios are considered as follows:

(i)   The daughter's half-life exceeds the parent's, $(T_{1/2})_D > (T_{1/2})_P$, resulting in $\lambda_D < \lambda_P$.

The ratio of Equation 2.25 reduces to:

$$\frac{A_D(t)}{A_P(t)} = \frac{\lambda_D}{\lambda_P - \lambda_D}\left[e^{(\lambda_D - \lambda_P)t} - 1\right] \qquad (2.26)$$

The ratio $A_D(t)/A_P(t)$ exponentially increases with time t, stipulating that no equilibrium between the parent and daughter activities [$A_P(t)$ and $A_D(t)$] will be attained.

(ii)   The half-life of the daughter is less than that of the parent: $(T_{1/2})_D < (T_{1/2})_P$ implying that $\lambda_D > \lambda_P$. The ratio $A_D(t)/A_P(t)$ at large t becomes a fixed value given as $\lambda_D/(\lambda_D - \lambda_P)$ as shown below:

$$\frac{A_D(t)}{A_P(t)} = \frac{\lambda_D}{\lambda_D - \lambda_P} = \text{const} > 1 \qquad (2.27)$$

the constant is time independent and larger than unity. Thus, signifying transient equilibrium.

(iii)   The daughter's half-life is much shorter than the parent's: $(T_{1/2})_D \ll (T_{1/2})_P$ or $\lambda_D \gg \lambda_P$. For time, t relatively large, the activity ratio $A_D(t)/A_P(t)$ of Equation 2.26 reduces to:

$$\frac{A_D(t)}{A_P(t)} \approx 1 \qquad (2.28)$$

i.e. $A_D(t) \approx A_P(t)$, the activity of the daughter $A_D(t)$ is approximately that of its parent $A_P(t)$, and they decay together at equal rates. This special scenario in which the parent and daughter activities are essentially identical is referred to as secular equilibrium (Ghoshal, 2014). A set of radioactive isotopes in decay chain series attain this equilibrium when the decay rate of parent radionuclide is equal to the

production rate of the daughter nuclides. The number of atoms of each species are constant (Bertulani, 2007). From equation 2.28, it is such that:

$$\frac{dN_1}{dt} = \frac{dN_2}{dt} = \cdots \cong 0$$

$$\Longrightarrow \lambda_1 N_1 = \lambda_2 N_2 = \lambda_3 N_3 = \cdots = \lambda_n N_n \tag{2.29}$$

Equation 2.27 is the generalised form of decay for successive radionuclide generations (1, 2, 3 up to nth) and is known as the Bateman's equation in secular equilibrium. It is employed in measuring the activity of a parent atom through the number of atom of daughter found in any generation. This is provided the radioactive sample attains secular equilibrium. The period is a minimum of 28 days for samples sealed in air-tight containment (Njinga *et al.*, 2015).

2.1.5 Interaction of radiation with matter

Radiation interactions depend on their type, mass electrical charge, energy as well as the constituent of the interacting medium (Cherry *et al.*, 2012). While passing through matter, radiations emitted during radioactive decay (charged particles and photons) transfer their energy. The principle mechanisms for the energy transfer are ionization and excitation of atoms and molecules (Cherry *et al.*, 2012). However, most of this energy degrades into heat (molecular and vibrations).

Alpha particles (^{4}He), due to their size, are slow and interact with atoms causing ionization and excitation. Ionization takes place when an outer electron of an atom is completely removed (Cherry *et al.*, 2012). Excitation takes place when the electrons are raised to a higher excited orbital. Though the initial energy of α-particles is reasonably high (3 to 8

Mev), their energy is dissipated very quickly and hence they are not very penetrating (Kakani and Kakani, 2008).

Beta particles with a negative charge (negatrons) are small compared to alpha particles and hence their interaction with matter is lesser (Ghoshal, 2014). Thus, they are more penetrating and moving rapidly causing ionization and excitation, though less than alpha particle. Beta radiation loses its energy in matter through ionization and generates electromagnetic radiation called bremsstrahlung (IAEA, 2003). Positrons passing through matter combine with electrons and produce two annihilation gamma quanta of energy 511 keV each.

Gamma rays are electromagnetic radiation (photons) and carry null charge or mass. Without appreciable energy dissipation, they travel very long distances. They are highly penetrating and produce secondary electrons while interacting with matter (Ghoshal, 2014). A minimal energy γ-ray can deposit all its energy to an orbital electron, causing it to be released from the atom as a photoelectron (photoelectric effect). A moderate energy γ-ray transfers only some portion of its energy to the orbital electron (which is then ejected) and further its motion with reduced energy (Cherry *et al*., 2012). The variation in energy between the impacting photon and the photon emitted can be determined as its wavelength change (Compton effect). A high energy γ-ray may excite a nucleus by transferring all its energy to the nucleus. The excited nucleus responds by emitting another photon of the same or lesser energy (Kakani and Kakani, 2008). This photon may further decay spontaneously to produce a positron-negatron pair (pair-production).

2.1.6 Health effects of radiation

Health effects are the biological implications of human exposure to radiations. Radiation effects vary with intensity of radiation dose absorbed by an individual and the duration of exposure, low dose rates occur when exposure is spread over an extensive time period, allowing affected cells sufficient time to repair damage to their DNA molecule (NYSDH, 2007). Hence, doses are less dangerous than when the same dose is instantly absorbed. Biological effects on cells arise from direct as well as indirect radiation action. Direct effects are produced by the instant action of the radiation itself while indirect effects are caused by the subsequent chemical action of free radicals and other radiation products (Turner, 2007).

Generally, health effects of radiation are grouped into two namely; threshold effects and non-threshold effects. They can occur as somatic (occurring in the person who receives the radiation dose), genetic (occurring in an exposed person's offspring) or terratogenetic (occurring in the offspring of individuals exposed during gestation) (Turner, 2007).

2.1.7 Threshold effects

High radiation doses received in a short of time lead to symptoms that can be observed shortly after exposure, certain dose range must be exceeded before occurrence. The severity of damage increases with the magnitude of the radiation dose received (NYSDH, 2007). Such effects are known as threshold (acute, deterministic or non-stochastic) effects. These include radiation sickness and death, cataracts, sterility, loss of hair, decreased thyroid function and radiation skin-burns. Table 2.2 below highlights threshold effects, accompanying symptom(s), dose limit/range of occurrence and associated risk to exposed individuals.

Table 2.2: Threshold effects of radiation

Threshold Effect	Symptoms of Exposed Population	Dose Limit (rem)	Risk
Radiation sickness	5% of exposed people may vomit	≈ 60	
	Rises to 50 %	≥ 200	
		300 - 400	Without medical treatment, death may occure at 50 % chance within 60 days
Cataracts	Clouding of the eye's lens	200 - 500	Blindness
Sterility	In men: Temporary sterility	≈ 15	
	Permanent sterility	400 – 500	Inability to procreate
	In women: Permanent Sterility	≥ 400	Infertility over 2 or 3 exposures

Source**:** NYSDH (2007)

2.1.8 Non-threshold effects

These are health effects of radiation that generally do not surface until long periods (years) after exposure, there are no threshold doses for these effects and any radiation exposure can increase a person's chances of having these effects (NYSDH, 2007). Non-threshold effects are also known as delayed (non-deterministic or stochastic) effects, they are random (statistically based), and with the chances of occurrence increasing with the magnitude of the dose but the severity does not (NYSDH, 2007). Non-threshold effects often occur as genetic or terratogenetic due to the time it takes for them to manifest. However, they are also somatic as in the case of a cancer patient suffering from radiation dose accumulated over prolong period of time.

2.2 Fundamentals of Gamma-ray Spectrometry

The gamma ray photon emitted by decaying radionuclides exhibit discrete energy. This energy is characteristic of the source radionuclide. Measurement of this energy is the gamma spectrometry basis (IAEA, 2003). Scintillation detectors are used in gamma spectrometry as their composite material emits light in response to incident gamma ray

photon. Incident radiation interacts with the atoms of the material and transfers some of their energy to the atoms which are excited to short-lived excited states. Relaxation of the excited states to the ground state results to emission of absorbed energy in the form of light (Ahmed, 2007). The intensity of the light emitted is proportional to the energy of the incident photon. A typical example of the scintillation material is a thalium-doped single crystal of sodium iodide, called NaI(Tl) (Raja and Barron, 2009). The NaI crystal is connected to a photomultiplier (PM) tube to convert small flashes of light into electrical signal. PM tubes are ultrasensitive electronic light detectors introduced to eliminate the counting speed and accuracy of the scintillation detectors (Cherry *et al.*, 2012). The experimental setup for the determination of the gamma radiation spectrum with a scintillation counter is shown in Figure 2.4.
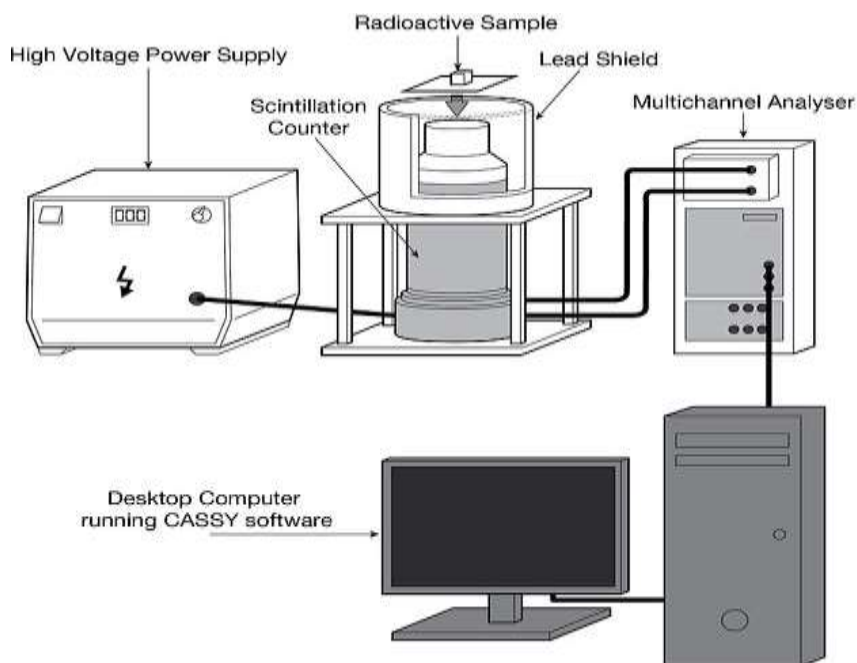
Figure 2.4: Experimental setup for determination of γ-radiation spectrum with a scintillation counter (Mustoe-Playfair, 2011)

Connected to the scintillation counter is a high voltage power supply. A Multi-channel Analyser (MCA) connected to the scintillation counter sends information to the computer.

Gamma spectroscopy measurements' accuracy and precision depends on data processing procedures, laboratory background shielding, geometry and mass of the sample, energy resolution and size of the detector, counting time and the quality of the radioactive standards (IAEA, 2003).

Semiconductors also accomplish the same effect as scintillation detectors. That is the altering of gamma radiation into electrical pulses. Although, through another route. In semiconductors, the energy gap between the conduction band and valence band of electrons is small (Raja and Barron, 2009). Gamma rays interact with a semiconductor material and impart sufficient energy to excite electrons to the band of conduction. Hence, altering the conductivity of the material and generating corresponding electrical signals that can be detected. The most common types are lithium-doped germanium crystals Ge(Li) and high-purity germanium (HPGe) detectors (Raja and Barron, 2009).

2.3 Mining Techniques and Artisanal Gold Mining in Nigeria

Generally, mining techniques are classified into surface and underground mining (Candeias *et al.*, 2018). Surface mining involves excavation done at the earth's surface while underground (or open pit) mining involves excavation of an area of overburden and removal of the ore exposed in the resulting pit. The goal of mining is to obtain desired minerals from excavation. This is achieved through the placer or in-situ methods. Placer method is applied to sieve out valuable metals from beach sands, sediments in river channels and other environments (AGI, 2019). *In-situ* mining, used mainly in uranium mining, it is an on-site dissolving of mineral resource and process it on the surface without the need for rock being displaced from the ground (AGI, 2019). Process employed depends

on the type of mineral resource being extracted, its location (surface or underground), environmental factors as well as cost-effective results (AGI, 2019 and Candeias *et al*., 2018). The impact on landscape and nearby environment also varies from one method to the other.

In Northern Nigeria, gold deposits are found most notably around old Birnin Gwari-Kwaga, Maru, Gurmana, Malele, Okolom-Dogondaji, Bin Yauri and Anka while in the South valuable deposits are found in Iperindo, Osun State (Okere, 2018). However, the Nation is yet to benefit from this wealth (21400 kg weight-worth in 2018) because of unliscensed mining and the shortfall of significant investors. Specifically, illegal mining contributes to the daily loss of about 100 kg (≈$9 billion yearly) (Okere, 2018). These miners are mostly artisans and may be unaware of the health and environmental implications mining. They use simple tools like shovels, pick-axes, pans, chisels and hammers. Plate I is a view of artisanal miners in Northern Nigeria and the simple tools used during excavation.

Plate I: Artisanal gold miners in Northern Nigeria (Okere, 2018)

In June, 2018, Professor Yemi Osinbajo (the Vice President of Nigeria) cautioned artisanal miners within the nation to abide by the mining rules to safeguard life and the environment

(Okere, 2018). He noted that, small-scale miners dominate the gold mining in Nigeria today. The self-evident consequences are exposure to significant hazards for miners, local community dwellers and the environment. Also, tailings resulting from mining operations may disperse and contaminate neighbouring communities. Such tailings are dense slush of waste materials left over after extraction of a commercially viable mineral from ore. They consist of pulverized rock, small amounts of metals, elements which are naturally harmful when exposed to air (Candeias *et al*., 2018). They are usually disposed-off on the surface of mining areas, in ponds in the form of dry stacks or piles. Therefore, diverging exposure into pathways that may enter the human food chain.

2.4 Review of Previous Studies

Several research interests have been inspired by the inhomogeneous distribution of NORM within the environment. Human exploits such as oil exploration and mining alter concentration magnitudes of NORM (Kamunda *et al*., 2016) and have resulted to environmental contamination and degradation. Global productions of mineral products have increased in recent years, resulting in processing of larger volumes of materials and with proportional negative environmental impacts (Jain *et al.*, 2016). The environmental and health implications of artisanal gold mining have kindled research interests. Several studies have been made in Nigeria and across the globe to assess the radiological implications of artisanal gold mining to the environment and occupationally exposed miners. Published studies on the concentration of NORM and implications to human health and environment are discussed below.

Darko *et al.* (2005) conducted preliminary studies on the occupational exposure to NORM from underground and surface mining in the Ashanti region (Ghana) gold mines. The assessments were performed using gamma spectrometry. The computerised system was coupled to a 3×3 squared inch NaI(Tl) measuring assembly. Employing the ICRP dose estimation methods, the annual effective doses were estimated to be 0.26 and 1.83 mSv for surface and subsurface mines respectively. The results obtained for surface mines were below the 1.00 mSv per year threshold while results for underground mines were above the 1.00 mSv per year stipulated threshold for workplace exposure (ICRP, 2007).

Natural background radioactivity of soil samples at the hotspot areas around Kinta District, Perak (Malaysia) were analysed by Kuan *et al.* (2009) using HPGe detector system. The soil activity ranged 43-307 Bq/kg for ^{238}U, 63-1377 Bq/kg for ^{232}Th and 29-166 Bq/kg for ^{40}K with mean values of 178, 841 and 104 Bq/kg respectively. Mean levels for ^{238}U and ^{232}Th indicate significant deposit of uranium and thorium within the observed area. Kuan *et al.* (2009) recommended that the data obtained can be used as a reference for comparison with future evaluations.

At the locality of two Minna (Nigeria) tertiary institutions, background radiations were assessed by *in-situ* measurements by Olarinoye *et al*. (2010). 34 points across the institutions were marked and assessed using a mobile radiation dosimeter (Geiger-Mueller tube-based). Dose rates obtained at Niger State College of Education Minna (NCM) varied from 0.13 to 0.17 μSv/h. Dose rates at the Federal University of Technology Bosso Campus (FUTB) varied from 0.15 to 0.18 μSv/h. While at the FUT Gidan-Kwano campus (FUTG) the dose rate was between 0.14 and 0.18 μSv/h. The mean dose rate for the surveyed points was 0.15 μSv/h with equivalent 0.19 mSv/y average annual effective dose. This value was

below the recommended 1.00 mSv/y stipulated by the ICRP for non-occupational population.

Odumo *et al.* (2011), radiologically surveyed and assessed some Migori gold minng sites (Macalder, Masara, Mikei, and Osiri) of southern Nyanza (Kenya). An innovative method employing a mono-channel Na(Tl) system was used to deduce the activities of ^{40}K and the progenies of ^{232}Th and ^{226}Ra. The radiation levels range widely from 80 to 413 Bq/kg, 12 to 145 Bq/kg and 21 to 258 Bq/kg for ^{40}K, ^{232}Th and ^{226}Ra, respectively. The deduced absorbed dose in air varied from 16 to 178 nGy/h (with 42 nGy/h average). While the radionuclides' activity concentration and the estimated annual absorbed dose were below the world's average, the amount of dust at the mines was quite high. The results obtained show that the artisanal miners are exposed to several levels of radionuclides and dust and calls for necessary precautions.

Faanu *et al.* (2011) conducted studies to assess the exposure of the public to NORM from the processing of gold ore from Tarkwa gold-mine in Ghana. Samples of water, dust, rock, and soil were examined employing Neutron Activation Analysis (NAA) and direct gamma spectrometry techniques. Sequentially, 15.2, 26.9 and 157.1 Bq/kg were the average activity concentrations for ^{238}U, ^{232}Th and ^{40}K in the soil/rock samples.. The mean activity concentrations measured in the dust samples were respectively 4.90 and 2.75 μBq/m^3 for ^{238}Uand ^{232}Th. The total annual effective dose to the public was estimated to be 0.69 mSv. Upon comparison with the world average value of 1 mSv/annum, Faanu *et al.* (2011) concluded that the results stipulate an insignificant public exposure from gold mining activities in Tarkwa.

From the State of Andhra Pradesh (India), Reddy *et al.* (2012) surveyed the extent of natural background radioactivity. This was aimed at establishing baseline radioactive data in the proposed uranium mining sites in the Lambapur and Peddagattu areas. ^{238}U activities in the depthless soil of the region ranged 100-176 Bq/kg, with a mean of 138.24 Bq/Kg. ^{232}Th ranged 64-116 Bq/Kg, with 83.15 Bq/kg average. The ^{40}K ranged 309-373 Bq/kg, with 343.20 Bq/kg mean. The mean radiation levels of ^{238}U and ^{232}Th in the study locations were observed to be quite with contrast to the Indian national as well as International averages.

Abdulkarim *et al*. (2013) scooped samples of soil from twelve sites within the Yankandutse artisanal gold mining belt in Kaduna State, Nigeria. The activities of ^{40}K, ^{226}Ra and ^{232}Th in the soil samples were determined using gamma ray spectroscopy method. The average concentrations of ^{40}K, ^{226}Ra and ^{232}Th in sequence were 382.01, 2.08 and 47.23 Bq/kg. The mean activity concentration of potassium and radium were below the UNSCEAR stipulated average of 400.00 and 35.00 Bq/Kg respectively while that of thorium was above the global average of 30.00. In the same year, Abdulkarim and Umar (2013) scooped twelve soil samples from the gold mining site of Tsofon-gwari (Colonial, Jiniya and Katsina) in Kaduna state. The observed samples contained insignificant amounts of ^{226}Ra and ^{40}K. Their activities varied with average values of 2.39 and 390.95 Bq/kg respectively while ^{232}Th in the soil varied with an average value of 51.98 Bq/Kg which was above global average (Abdulkarim and Umar, 2013). Hence, indicating significant thorium levels in the soil. For the same region, Nasiru *et al*. (2013) investigated the activity concentrations of naturally occurring radionuclides (^{238}U, ^{232}Th and ^{40}K) in gold ore mined from Birnin Gwari artisanal goldmine. Instrumental Neutron Activation Analysis (INAA) technique

was employed in this case. Twelve samples were collected from pits at different depths. The activity concentration due to ^{238}U ranged from 6.18±3.7 to 66.69±4.9 Bq/Kg with 37.36±5.45 Bq/Kg mean, ^{232}Th concentrations ranged from 16.65±0.8 to 87.29±1.2 Bq/Kg with 62.69 ± 6.33 mean and ^{40}K range from 85.13±4.5 to 1564.69±57.9 Bq/Kg with a mean value of 997.52±11 9.97 Bq/Kg. These results revealed high levels of radioactivity within the gold mine. Thus, gold mining in the area poses radiological risks to miners and members of the public.

Aimed at identifying and quantifying fore-standing gamma-emitting NORM associated with mining activities in Northwestern Nigeria, Innocent *et al*. (2013) collected soil samples from 10 different mining sites in Zamfara State for gamma spectroscopy analysis. A laboratory based γ-ray NaI(Tl) system was used to obtain values of activity concentration ranging from 227.10 ± 7.54 to 590.44 ± 10.57, 4.68 ± 3.52 to 18.98 ± 0.84 and 40.58 ± 1.85 to 94.92 ± 2.75 Bq/kg for ^{40}K, ^{238}U and ^{232}Th respectively. The absorbed dose rate in the soil sample ranged from 9.47 ± 0.31 to 24.62 ± 0.44, 2.16 ± 1.62 to 8.77 ± 0.39 and 24.51 ± 1.12 to 57.33 ± 1.66 nGy/h respectively for ^{40}K, ^{238}U and ^{232}Th. The net absorbed dose rate estimated for the sites was 59.70 nGy/h and the estimated annual effective dose for the study ranged from 52 to 106 μSv/y, with an average of 73 μSv/y (Innocent *et al.*, 2013). Thus, revealing that the radiation exposure level for members of the public in the study areas is within the safety limit.

Doyi *et al.* (2013) carried out measurements of radon and gamma radiation levels in the underground artisanal gold mines in Tongo, Ghana. Solid State Nuclear Track Detectors (SSNTD) were used to estimate the mean ^{222}Rn concentration and dose rates during the Harmattan season (from November, 2010 to February, 2011). The measurements obtained

for ^{222}Rn concentrations were less than the action level of 500 Bq/m^3 recommended by ICRP for workplaces. The activity concentrations of ^{40}K, ^{232}Th and ^{238}U were determined using gamma-ray spectroscopy method. Average specific activities due to ^{238}U, ^{232}Th and ^{40}K for the mining sites were 66.29, 294.43 and 1964.29 Bq/kg in sequence. Therefore, revealing significant radiation levels above UNSCEAR (2000) stipulated average.

Ibrahim *et al*. (2013) used using Sodium Iodide-Thallium Gamma Spectroscopy to determine ^{226}Ra, ^{232}Th and ^{40}K natural activity concentrations in some mining areas in Central Nasarawa State, Nigeria. 21 soil samples were collected from the accessible areas of 7 major sites identified as the most mined areas of the zone. The mean activity concentrations were 32.52±4.65, 56.23±2.30 and 403.96±7.29 Bq/kg for ^{226}Ra, ^{232}Th and ^{40}K respectively. The value obtained for ^{226}Ra was a bit lower compared to world average while values for ^{232}Th and ^{40}K were higher than the world average value. The average background radiation absorbed doses at two spots were 5.81±0.08 and 8.45±0.56 mSv/y. These were higher compared to worldwide average of 1.00 mSv/y stipulated by UNSCEAR (2000).

From the gold mining area in Itagunmodi, Osun State of south-western Nigeria, the specific activities of NORM in soil samples were measured by gamma spectrometry using Sodium Iodide detector by Ademola *et al.,* (2014). The average activity concentrations of ^{238}U, ^{232}Th and ^{40}K determined in the soil from the mining sites were 55.3, 26.4 and 505.1 Bq/kg respectively. Except for ^{232}Th, these values are above UNSCEAR global average. However, lower radiation levels were recorded in the normal living with mean values of 8.8±1.9, 17.5±2.7 and 102.8±12.1 Bq/kg for ^{238}U, ^{232}Th and ^{40}K in sequence. The averages for radium equivalent activity concentration, external and internal hazard indices in the study

area were below the world averages. According to Ademola *et al.* (2014), mining activities in Itagunmodi poses no radiological hazard to the general public.

Girigisu *et al.* (2014) assessed the radiation levels from Awwal artisanal gold mining exercises in Kebbi State. Results reveal average activities of 23.85 ± 2.01, 18.80 ± 1.21 and 425.96 ± 5.56 Bq/Kg for ^{226}Ra, ^{232}Th and ^{40}K respectively. The average outdoor gamma dose was 34.26 nGy/h while the mean annual effective dose rate was 0.042 mSv/year which is less than 1.00 mSv/year benchmark given by UNSCEAR (2000). Radiologically, the values obtained are low and do not imply any significant health concerns to the local population. However, Girigisu *et al.* (2014) reported that they were unprofessional practices such as ignoring the use of gas mask while working in the dust-filled mine cafes and at the mills. This could also potentially expose workers to risks from inhalation of respiratory crystalline silica radon gas. The specific activities of ^{238}U, ^{232}Th and ^{40}K were measured in 60 soil samples by Al-Gazaly *et al.* (2014) using a NaI(Tl) gamma-ray spectrometry system. The samples were collected from sites around the uranium mine in the Abu-Skhair in Najaf province, Iraq. Computed mean values for ^{238}U, ^{232}Th and ^{40}K specific activities were 77.33, 9.36 and 426.31 Bq/kg respectively. The study also examined radium equivalent (Ra$_{eq}$) with an average of 123.54 ± 8.88 Bq/kg. A comparison of the measured values with the corresponding worldwide average values shows that the most specific activity of ^{238}U and ^{40}K radionuclides in the studied samples were higher than world average activity values.

Aliyu *et al.* (2015) radiologically surveyed selected mining sites (Kumar barite, Akiri copper, Azara barit, Ribi barite, Adudu lead, Keana salt and the Abuni zinc mines) in Nigeria's home of solid minerals (Nasarawa State). The activity concentrations of

primordial radionuclides (^{226}Ra, ^{232}Th and ^{40}K) in the surface soils/sediment samples were determined using sodium iodide-thallium gamma spectroscopy. The result shows that the activity concentrations of ^{40}K were higher than the world average. However, the annual effective dose rates (in mSv/y) were less than unity for all the mines. The external hazard indices for all the mines were less than unity. Thus, indicating minimal radiological risks associated with mining in the State.

Kamunda *et al*. (2016) evaluated the radiological hazards associated with exposure to NORM from gold mine tailings in the province of Gauteng in South Africa using gamma spectroscopy to measure activity concentrations in 56 soil samples from the mine tailings and 10 soil samples from a control area. The average activity concentrations in Bq/kg for ^{238}U, ^{232}Th, and ^{40}K from the mine tailings were found to be 785.3 ± 13.7, 43.9 ± 1.0 and 427.0 ± 13.1 respectively while the average activity concentrations from the control area in Bq/Kg were found to be 17.0.1 ± 0.4, 22.2 ± 0.5 and 496.8 ± 15.2 for ^{238}U, ^{232}Th, and ^{40}K respectively. Radiological hazard parameters calculated from these activity concentrations were higher than recommended safe limits (Kamunda *et al.*, 2016). In particular, average values for the external hazard (H_{ex}) and the internal hazard (H_{in}) from the mine tailings were 2.4 and 4.5 respectively. Both values were higher than unity, posing a significant health risk to the population in the area.

Nwankpa *et al.* (2016) also assessed 20 samples of soil from different illegal gold mines in Erinmo, Osun State of Nigeria. HPGe detector was used to quantify NORM in the soil. Radiation levels vary from 9.01±1.7 to 35.4±3.7, 10.9±2.8 to 37.5±4.6 and 99.0±12.3 to 182.8±18.5 Bq/Kg for ^{238}U, ^{232}Th and ^{40}K in sequence with averages of 21.9±2.1, 23.4±2.9 Bq/Kg and 136.5±18.2 Bq/Kg respectively. Hence, it was opined by Nwankpa *et al.* (2016)

that there were no uranium or thorium deposit in Erinmo due to uranium and thorium specific activities that fall within the earth crustal mean for normal environmental. Estimated radiological parameters were also below global threshold values, indicating minimal radiological contamination in Erinmo mines.

Radionuclides concentration in the surface soil of the uranium mining area of Tongliao, China, were investigated by Haribala et al. (2016). Using gamma spectrometry, the estimated average activity concentrations of ^{238}U, ^{232}Th, ^{226}Ra, ^{40}K and ^{137}Cs were 27.53, 15.89, 12.64, 746.84 and 4.23 Bq/kg respectively. Except for ^{40}K, these values were below recorded global averages. The averages for absorbed dose rate in the air, annual effective dose, radium equivalent activity, external and internal hazard indices computed were all within the bearable limits.

Faanu et al. (2016) ascertained the levels of NORM in the new eastern concession area of Perseus Mining (Ghana) Limited. This was done prior to processing of gold ore within and around the region. The study was based on situ measurements of external gamma dose rate at 1 m above ground level as well as laboratory analysis by direct gamma spectrometry to quantify ^{238}U, ^{232}Th and ^{40}K in soil samples. The average absorbed dose rate was determined to be 0.08 μGy/h. Individually, the mean concentrations of ^{238}U, ^{232}Th, and ^{40}K in the soil were 65.1, 71.8 and 1168.3 Bq/Kg. These values were all above the UNSCEAR (2000) reported global average and results to an annual effective dose of 0.91 mSv/yr that was slightly below the 1.00 mSv threshold for public exposure. It was the opinion of Faanu et $al.$ (2016) that previous mining activities had not imparted negatively in terms of radiological hazard to the communities in this area. However, these results suggest

concerns for further radiological evaluation and monitoring in consideration miners health and environmental safety.

Silver *et al.* (2016) assessed the levels of primordial radionuclides in mine tailings from mines in Southwestern Uganda. The specific activity concentrations of ^{238}U, ^{232}Th and ^{40}K in the samples varied from 35.5 to 147.0 Bq/Kg, 119.3 to 376.7 Bq/Kg and 141.0 to 1658.5 Bq/Kg respectively. The mean absorbed dose rates in sequence for Mashonga Gold Mine, Kikagati Tin Mine and Butare Iron Ore mine were 181.2, 167.2 and 191.6 nGy/h. These values were more than three times the world wide average value of 57 nGy/h. Thus, Silver *et al.* (2016) suggested that the mine tailings (soil) from these areas should not be used as major building material to minimize radiological hazards (Silver *et al.*, 2016).

Radionuclides activities in soils in the vicinity of 10 solid mineral mining sites in Enugu, Nigeria were investigated by Osimobi *et al.* (2018). Sodium iodide gamma spectroscopy was used to assess 4 soil samples and 1 control sample obtained from each of the sites. The results obtained indicated mean concentration values of 33.2, 77.7 and 100.7 Bq/kg for ^{226}Ra, ^{232}Th and ^{40}K in sequence. The averages deduced for the radiological risk parameters were 67.5 ηGy/h for the Absorbed Dose Rate (DR), 82.8 μSv/y for the Annual Effective Dose Equivalent (AEDE), 151.4 Bq/Kg for the Radium Equivalent (Raeq) and 457.1 mSv/y for the Annual Gonadal Equivalent Dose (AGED) which was high compared to the control value of 177.7 mSv/y and the WHO tolerable value of 300 mSv/y.

Gamma-ray spectrometry using NaI(Tl) detector was employed by Ibraheem *et al*. (2018) to determine NORM concentrations in the Asir region of Saudi Arabia. Soil samples assessed were fetched from several locations (Muhail Asir, Abha and Khamis Mushait)

within the area. The results show the variations of NORM concentrations from 38.2±0.1 to 44.1±0.1, 23.49±0.20 to 41.9±0.2 and 182.5±1.0 to 251.5±1.3 Bq/Kg for ^{226}Ra, ^{232}Th and ^{40}K respectively. Estimated averages were all below the UNSCEAR (2000) stipulated global average. According to Ibraheem *et al*. (2018), the data obtained will serve as baseline level of radionuclides that occur naturally in the study area. Also, the results will be useful for tracking and evaluating pollution inventory within the boundaries of the surveyed areas.

Suleiman *et al.,* (2018) reported minimal level of radiation exposure around Erena mining sites in Niger State, Nigeria. 7 soil samples were collected and analysed using a laboratory NaI(Tl) γ-ray spectrometer at the Centre for Energy Research and Training (CERT), Ahmadu Bello University Zaria. The activity concentrations for ^{40}K ranged from 48.52±3.58 to 1002.96±9.80 Bq/Kg, for ^{226}Ra it ranged from 23.29±2.20 to 75.32±5.09 Bq/Kg and for ^{232}Th the range was from 23.83±2.05 to 59.29±2.39 Bq/Kg. However, the mean values of activity concentrations and radiological parameters were below the global screening levels. Therefore, Suleiman *et al.,* (2018) suggested that no radiological risk was envisaged to the populace of the study areas and the miners working on the mining sites.

Using Radiation Inspector Alert meter (EXP+ model), measurements were made at four different Stations (A, B, C and D) within the vicinity of artisanal gold mining sites in Luku, Niger state by Sabo *et al.,* (2018). The investigation revealed averages 1.66, 1.5, 1.48 and 2.12 mSv/yr respectively for stations A, B, C and D. The radiation levels recorded from the sampling stations exceeded the 1.00 mSv/yr threshold set by the International Commission for Radiological Protection (ICRP) for public exposure. Thus, indicating that the community is at risk of exposure to high radiation dose resulting from artisanal gold mining

activities. In reducing radiation emissions and their resulting harm to the community, Sabo *et al.,* (2018) recommended the adoption of strict regulations and enforcement of mining policies such as the 2007 Minerals and Mining Act that formally disallowed illegal exploration and/or exploitation of Minerals.

Saïdou *et al.* (2019) investigated natural radiation exposure and its health effects in mining and ore bearing regions of Cameroon from 2014 to 2017. Air kerma rates were measured using car-borne survey method. The air kerma rate range between 25–102, 28–71, 23–80 and 34–102 nGy/h in Poli, Lolodorf, Betare-Oya and Douala. The corresponding mean air kerma rate was 57, 47, 44 and 65 nGy/h respectively in the aforementioned regions. The average value of in Poli and Douala city were found to be equal and higher than the world average value of 57 nGy/h given by UNSCEAR (2000). In-situ gamma spectrometry was used to determine activity concentrations of ^{238}U, ^{232}Th and ^{40}K in soil. The highest activity concentrations of ^{238}U, ^{232}Th and ^{40}K were found in the uranium and thorium bearing region of Lolodorf. According to Saïdou *et al.* (2019), natural radioactivity level seems to be normal in most of the surveyed areas. However, there are many points where activity concentrations of natural radionuclides are largely above the world average values.

Natural radioactivity at separate locations of the uranium-rich zones of Lambapur-Peddagattu and Seripally areas in Telangana state, India were assessed by Raghavendra *et al.* (2019). The average activity concentrations of 48.07±22.30, 230.77±89.26 and 807.08±255.87 Bq/kg were observed for ^{238}U, ^{234}Th, and ^{40}K in the soil respectively. The annual effective dose was realised to be comparable with similar studies in India and the several regions of the globe.

Published results reviewed have shown an uneven distribution of NORM across different regions with several values recorded below globally estimated averages. Such results indicate insignificant amount of the specified radionucludies while those above the global average indicated significant deposits of radionuclides in the observed region. Values for radiological parameters above threshold values stipulated by the UNSCEAR (2000) imply radiological implications of artisanal gold mining and other human activities occurring in the said region. Thus, signifying the need for environmental monitoring, regulation and control because exposure to radiations, no matter how small the doses are, poses radiological risks to man and the environment. This review also buttresses the need for evaluations to assess the radiological impact of artisanal gold mining in regions where radiological parameters have not been measured.

CHAPTER THREE

3.0 MATERIALS AND METHOD

3.1 Sampling Site

The sample site is Gababiyu artisanal goldmine in Minna Metropolis. Minna is the capital city of Niger State, Nigeria and situated between 6°25' E and 6°45' E longitude and latitude 9° 24' N and 9° 48' N. Two key rock formations (the basement complex and sedimentary rocks) cover the State. To the south of the State, there are sedimentary rocks characterised by alluvial deposits and sandstones, especially along the Niger valley and in most of the Agaie, Bida, Borgu, Gbako, Lapai, Lavun, Mokwa and Wushishi LGAs (Ajibade, 1976 and Olarinoye *et al.*, 2010). This sub-area also includes vast Niger River flood plains, making the state one of the largest and most fertile agricultural lands in the country (Ajibade, 1976 and Olarinoye *et al.*, 2010). The basement complex is to the north, distinguished by inselbergs (outcrops of granite) that occur in rolling landscape's expansive topography. In Gurara, Mariga, Minna, Rafi and Shiroro LGAs, these inselbergs dominate the landscape (Ajibade, 1976 and Olarinoye *et al.*, 2010). The map of Niger State, Nigeria is shown in Figure 3.1 with the capital city of Minna located between Bosso and Chanchaga LGAs. The study area is further shown in Minna. The mining site is off the city's eastern bye-pass, after the M. I. Wushishi estate.
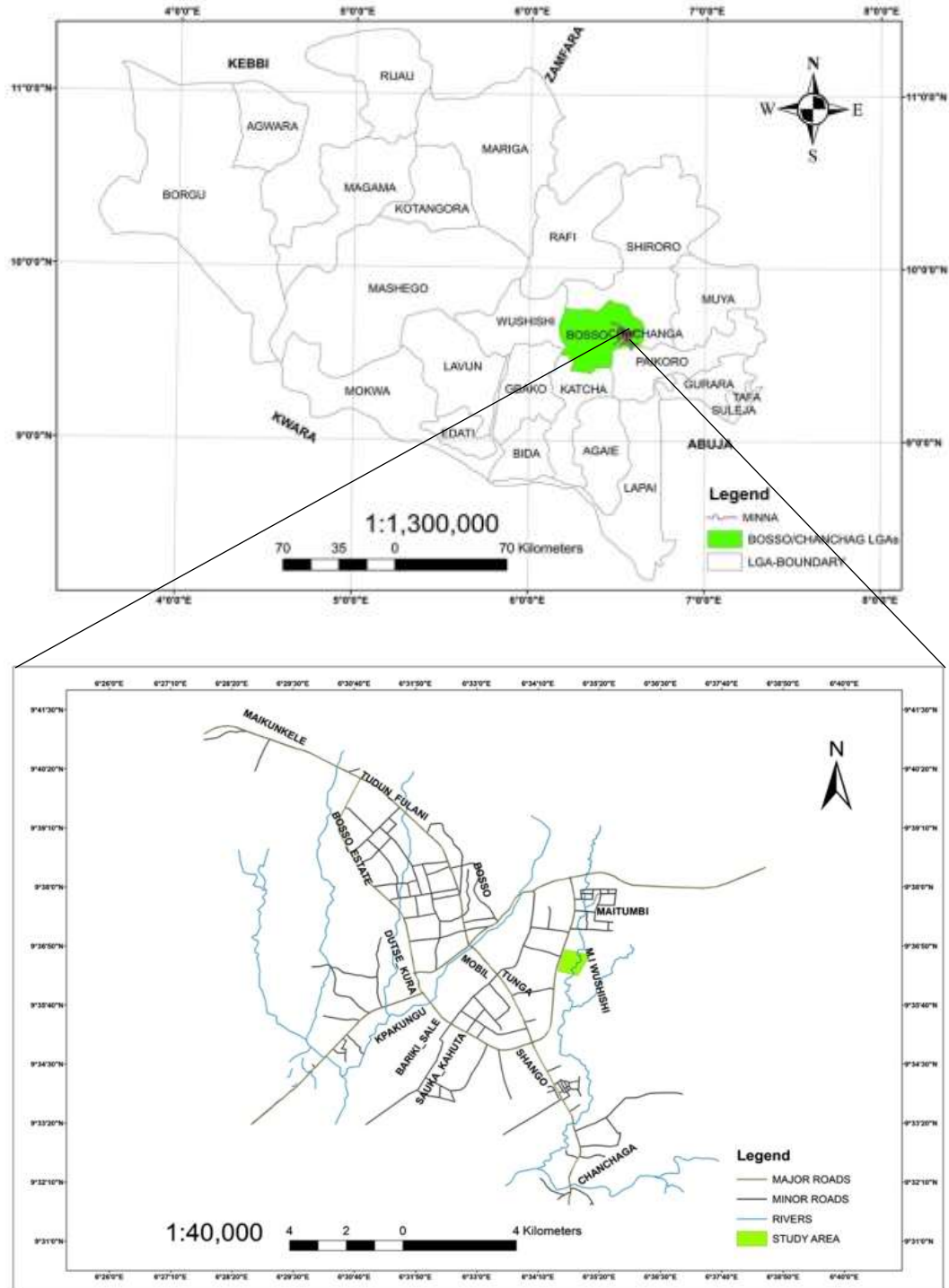
Figure 3.1: Location map of Minna in Niger State, Nigeria
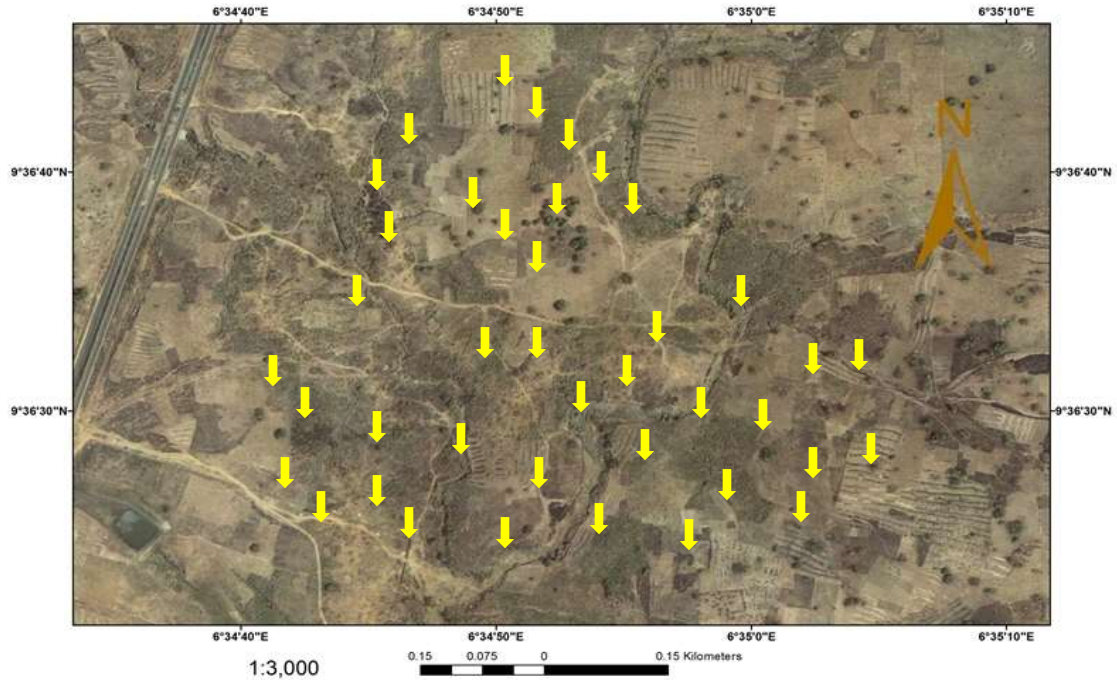
Figure 3.2: Sampling points in Gababiyu mining area

Plate II describes views of the area where a miner uses the placer method along the tributaries of the River Chanchaga. The miner in Plate II is without any protective gear and therefore exposed to toxic matter.

Plate II: Artisanal miner in Gababiyu goldmine, Minna

3.2 Collection of Sample and Preparation

Forty surface-soil samples were collected around Gababiyu artisanal goldmine in Minna Metropolis. The sampling points were selected based on accessibility and closeness to mining pits where tailings are present. The mining pits are points from which gold have been crudely mined. The collection points were marked "GM01 to GM40" and their locations tagged using GPS. Table 3.1 shows the collected sample ID and their corresponding GPS locations.

1.00 ± 0.10 kg of soil samples were fetched from the selected points (indicated in Figure 3.2). The samples were collected into polyethylene bags labeled "GM01 to GM40" accordingly with the sample ID locations and conveyed for preparation at the laboratory.

Each of the soil samples were air-dried in the Applied Nuclear Physics Laboratory, Federal University of Technology Minna to strip them of their quality in humidity (Kolo *et al.*, 2019). The dry samples were crushed samples and filtered with a sieve of BSS 63 aperture ($\approx$250 micron mesh size) to obtain uniformly homogenous sample matrix with improved surface area to volume ratio. 500.00 ± 0.10 g of the sieved samples were loaded in well labeled polyethylene bag and transferred to the Centre for Energy Research and Training (CERT) Zaria for radiometric analysis. At CERT laboratory, 300.00 ± 0.10 g of each sample was re-packaged in 7.6 cm $\times$ 7.6 cm radon-impermeable cylindrical plastic containers. To ensure that the containers were air-tight to prevent ^{222}Rn from escaping, the containers were each triple sealed. The sealing procedure was achieved by smearing of each container's inner rim with Vaseline jelly, filling the lid gap with candle wax to cover the holes between lid and container, and firmly sealing lid containers with masking tape.

Table 3.1: Sample ID and GPS location of the collected soil samples

S/N	Sample ID	Coordinates	
		Longitude	Latitude
1	GM 01	06º 34' 40.9"	09º 36' 39.5"
2	GM 02	06º 34' 40.4"	09º 36' 38.2"
3	GM 03	06º 34' 39.6"	09º 36' 39.1"
4	GM 04	06º 34' 40.0"	09º 36' 39.8"
5	GM 05	06º 34' 40.0"	09º 36' 40.5"
6	GM 06	06º 34' 40.2"	09º 36' 40.4"
7	GM 07	06º 34' 41.7"	09º 36' 40.4"
8	GM 08	06º 34' 42.7"	09º 36' 40.1"
9	GM 09	06º 34' 43.2"	09º 36' 39.5"
10	GM 10	06º 34' 43.3"	09º 36' 38.6"
11	GM 11	06º 34' 45.8"	09º 36' 39.4"
12	GM 12	06º 34' 45.4"	09º 36' 40.4"
13	GM 13	06º 34' 44.2"	09º 36' 39.5"
14	GM 14	06º 34' 43.8"	09º 36' 39.1"
15	GM 15	06º 34' 44.2"	09º 36' 38.9"
16	GM 16	06º 34' 45.0"	09º 36' 38.1"
17	GM 17	06º 34' 42.9"	09º 36' 36.8"
18	GM 18	06º 34' 42.3"	09º 36' 37.6"
19	GM 19	06º 34' 42.5"	09º 36' 37.6"
20	GM 20	06º 34' 42.5"	09º 36' 37.3"
21	GM 21	06º 34' 53.6"	09º 36' 31.0"
22	GM 22	06º 34' 53.3"	09º 36' 30.6"
23	GM 23	06º 34' 50.9"	09º 36' 31.2"
24	GM 24	06º 34' 54.4"	09º 36' 30.8"
25	GM 25	06º 34' 53.9"	09º 36' 31.2"
26	GM 26	06º 34' 54.1"	09º 36' 30.8"
27	GM 27	06º 34' 53.5"	09º 36' 30.7"
28	GM 28	06º 34' 53.8"	09º 36' 30.8"
29	GM 29	06º 34' 53.8"	09º 36' 31.0"
30	GM 30	06º 34' 53.1"	09º 36' 30.5"
31	GM 31	06º 34' 53.6"	09º 36' 31.6"
32	GM 32	06º 34' 50.6"	09º 36' 31.2"
33	GM 33	06º 34' 53.8"	09º 36' 31.4"
34	GM 34	06º 34' 42.2"	09º 36' 32.3"
35	GM 35	06º 34' 43.2"	09º 36' 32.0"
36	GM 36	06º 34' 43.4"	09º 36' 31.6"
37	GM 37	06º 34' 42.7"	09º 36' 32.1"
38	GM 38	06º 34' 41.3"	09º 36' 29.9"
39	GM 39	06º 34' 42.0"	09º 36' 32.0"
40	GM 40	06º 34' 41.8"	09º 36' 30.7"

Plate III is a display of the packaged 500.00±0.10 g samples and the detector volume-sized plastic into which they were contained. The sealed samples were stored for 28 days to enable radon and its short-lived descendants achieve secular equilibrium (Girigisu *et al*., 2014) prior to gamma spectrometric analysis.

Plate III: Packaged 500 g samples and the detector volume-sized plastic container

3.3 Sample Analysis

Gamma spectrometry was employed for sample analysis using a 7.6 by 7.6 cm^2 NaI (Tl) detector crystal connected optically to a photomultiplier tube (PMT). The assembly does have one incorporated preamplifier and outsource of 1 KV. To mitigate the effects of scattered and background radiations, the detector was wrapped in a 6 cm cadmium and copper sheets with lead shield. Canberra Nuclear Products' (800 Research Parkway Meriden, Connecticut, United States) Maestro is the data acquisition program used for spectrum analysis.

Two calibration point sources (^{137}Cs and ^{60}Co) were used to perform the calibration of the system for energy before sample analysis. These were achieved with the amplifier gain

which gives energy resolution of 72% for the 661.16 KeV of ^{137}Cs, and counting done for 30 minutes. Calibration standards used for checking the calibration were the IAEA gamma spectrometric reference materials RGU-1 for ^{226}Ra (^{214}Bi peak), RGTh-1 for ^{232}Th (^{208}Ti peak) and RGK-1 for ^{40}K. The energy peak for ^{226}Ra ^{232}Th and ^{40}K identified in the spectrum with their respective energy windows are shown in Table 3.2.

Table 3.2: Spectral energy windows used in the analysis

Isotope	Gamma energy (KeV)	Energy window (KeV)
^{226}Ra	1764.0	1620-1820
^{232}Th	2614.5	2480-2820
^{40}K	1460.0	1380-1550

The system was set at 0–3000 KeV working limit to accommodate the energy range of being studied. The IAEA standard sources shown in Table 3.3 were used to determine the absolute detection efficiency of the detector. The system energy calibration curve using ^{137}Cs and ^{60}Co point sources is shown in Figure 3.3.

Table 3.3: Typical standard gamma-ray sources

S/N	Source	Half-life ($T_{1/2}$) (Years)	Gamma Energy (MeV)
1	^{60}Co	5.26	1.173 and 1.332
2	^{137}Cs	30.00	0.662
3	^{54}Mn	312.50	0.835
4	^{133}Ba	10.52	0.340 and 0.081
5	^{22}Na	2.60	0.511 and 1.275

Source: (Njinga *et al.*, 2015 and Varier, 2009)
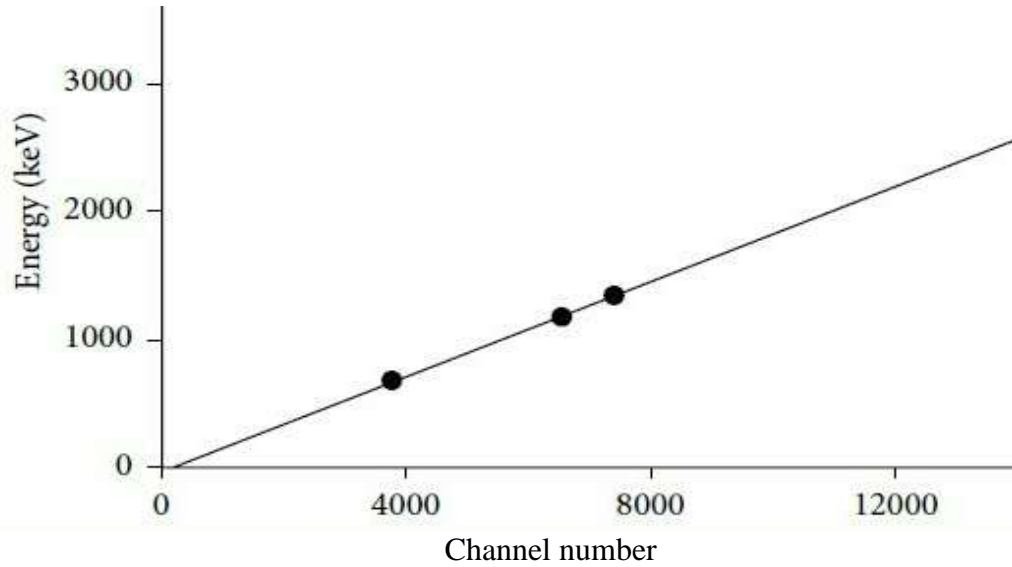
Figure 3.3: Energy calibration curve for the Na(Tl) detector

Each of the samples was measured for a period of 29000 seconds ($\approx$8 hours). The area of each energy peak in the spectrum was used to compute the activity concentrations of each radionuclides of interest in the sample by employing following equation (Njinga *et al.*, 2015):

$$A_i \ (Bq.\,kg^{-1}) = \frac{C_n}{I_{(\gamma)}\varepsilon MT} \qquad (3.1)$$

where, A_i is the activity concentration of a particular radionuclide in the sample,

C_n is the count rate (counts per second),

$I_{(\gamma)}$ is the emission probability of a specific energy photo peak,

ε is the absolute efficiency of the detecting system,

T is the sample counting time, and

M is the mass of the sample in kg.

The C_n, was obtained using the equation:

$$\text{count per second (cps)} = \frac{\text{Net count}}{\text{Live time}}, \qquad (3.2)$$

3.4 Radiological Parameters

From the specific activity obtained from Equation 3.1, radiological parameters were computed using appropriate model. The parameters are equivalent radium activity, gamma radiation dose, annual equivalent effective dose, annual equivalent gonadal dose, activity utilization index, external and internal hazard indices, representative gamma index and excess lifetime cancer risk. They were estimated to assess the radiological implication of artisanal gold mining in Gababiyu.

3.4.1 Radium equivalent activity

The Radium Equivalent Activity (Ra_{eq}) is the weighted sum of hazards associated with ^{226}Ra, ^{232}Th and ^{40}K. This index presumes that 1, 0.7 and 13 Bq/Kg of ^{226}Ra, ^{232}Th and ^{40}K produce equal terrestrial gamma dose rates (Berekta and Mathew, 1985; Kolo *et al.*, 2019 and UNSCEAR, 2000). UNSCEAR (2000) stipulates a threshold of 370 Bq/kg for Ra_{eq} (Suleiman *et al.*, 2018). Ra_{eq} was estimated using Equation 3.3 (Kolo *et al.*, 2019 and Osimobi *et al.*, 2018):

$$Ra_{eq} = \left(\frac{A_{Ra}}{370} + \frac{A_{Th}}{259} + \frac{A_K}{4810}\right) 370 \text{ Bq/Kg} \tag{3.3}$$

where, A_{Ra}, A_{Th} and A_K are respectively the specific activity concentrations of ^{226}Ra, ^{232}Th and ^{40}k in the soil samples.

3.4.2 Gamma radiation dose

The gamma radiation dose or absorbed dose (D) one metre above ground was estimated using the relation (Munyaradzi *et al.*, 2018 and UNSCEAR, 2000):

$$D = 0.462A_{Ra} + 0.604\ A_{Th} + 0.0417A_K \tag{3.4}$$

where, D is the gamma radiation dose in nGy/h and A_{Ra}, A_{Th} and A_K are the activity concentrations of ^{226}Ra, ^{232}Th and ^{40}K in sequence. The coefficients in Equation 3.4 (0.462, 0.604 and 0.0417 in nGy/h per Bq/Kg) are the dose conversion factors for ^{226}Ra, ^{232}Th and ^{40}K respectively (Munyaradzi, *et al.*, 2018 and UNSCEAR, 2000).

3.4.3 Annual effective dose equivalent

Annual Effective Dose Equivalent (AEDE) in mSv/y is estimated as products of the gamma radiation dose, D (nGy/h), time in a year (8760 hours), dose conversion factor of 0.7 Sv/Gy and occupancy factor (F) for outdoor exposure (Taskin *et al*., 2009 and UNSCEAR, 2000).

$$\text{AEDE} = D \times 8760 \times 0.7 \times F \times 10^{-6} \tag{3.5}$$

Occupancy factor of 0.375 (37.5 %) was employed in this study to account for the 9 hours the miners spend on the field per day,

3.4.4 Annual gonadal dose equivalent

The annual gonadal dose equivalent (AGDE) is a measure of the dose received by the gonads (gamete producing organs) of exposed population in a year (Kolo *et al.*, 2015 and Morsy *et al.*, 2012). AGDE was calculated using Equation 3.6 (Chandrasekaran *et al.*, 2014 and Kolo *et al*., 2019)

$$\text{AGDE}(\mu\text{Sv.y}^{-1}) = 3.09A_{Ra} + 4.18A_{Th} + 0.314A_K \tag{3.6}$$

where, A_{Ra}, A_{Th} and A_K assume their respective definitions as earlier stated.

3.4.5 Activity utilisation index

Activity Utilisation Index (AUI) is the parametric model used in determining NORM dose levels in the atmosphere from soil samples (Osimobi *et al*., 2018). AUI was calculated from

the specific activities of ^{226}Ra, ^{232}Th and ^{40}K in the sampled soils using the equation (Osimobi *et al*., 2018 and Sivakumar *et al*., 2014):

$$\text{AUI} = \left(\frac{A_{Ra}}{50 Bq/Kg}\right) f_{Ra} + \left(\frac{A_{Th}}{50 Bq/Kg}\right) f_{Th} + \left(\frac{A_K}{500 Bq/Kg}\right) f_K \qquad (3.7)$$

where, f_{Ra}, f_{Th} and f_K with numerical values of 0.462, 0.604 and 0.041, respectively, represent entire gamma dose fragmentary supplements for ^{226}Ra, ^{232}Th and ^{40}K (Kolo *et al.*, 2019 and Chandrasekaran *et al*., 2014).

3.4.6 External and internal hazard indices

External hazard index (H_{ex}) is a parameter used for evaluation of external exposure to gamma radiation in air. The maximum allowed value for H_{ex} is 1, corresponding to the upper limit of Ra_{eq} (370 Bq/kg) (Stranden, 1976 and Suleiman *et al*., 2018). Internal hazard index (H_{in}) on the other hand is a factor used to evaluate the hazardous effects of radon and its short-lived lineage to the organs of respiration (Suleiman *et al.*, 2018). The threshold for H_{in} is also 1.

The external hazard index (H_{ex}) and internal hazard index (H_{in}) were estimated using Equations 3.8 and 3.9 respectively (Berekta and Mathew, 1985 and Osimobi *et al*., 2018):

$$H_{ex} = \frac{A_{Ra}}{370} + \frac{A_{Th}}{259} + \frac{A_K}{4810} \leq 1 \qquad (3.8)$$

$$H_{in} = \frac{A_{Ra}}{185} + \frac{A_{Th}}{259} + \frac{A_K}{4810} \leq 1 \qquad (3.9)$$

3.4.7 Representative gamma index

Representative gamma index ($I_{\gamma r}$) is used to evaluate the conformity of soil to dose standards set for building materials (Jibiri *et al.*, 2014 and Kolo *et al.*, 2019). It categorises materials that may induce radiological risk if deployed for construction (Osimobi *et al.*,

2018). $I_{\gamma r}$ was computed from the equation (Ashraf et $al.$, 2010 and Osimobi et $al.$, 2018):

$$I_{\gamma r} = \frac{A_{Ra}}{150} + \frac{A_{Th}}{100} + \frac{A_K}{1500} \qquad (3.10)$$

$I_{\gamma r}$ must be ≤ 1 to achieve the given dose criteria which corresponds to an annual effective dose below 1 mSv (Kolo et $al.$, 2019 and Osimobi et $al.$, 2018).

3.4.8 Excess lifetime cancer risk

Excess Lifetime Cancer Risk (ELCR) is a measure of the probability that a certain stochastic effect will occur in an individual exposed to low doses of ionizing radiation over a given period of time (Silver et $al.$, 2016 and UNSCEAR, 2000). The most prominent radiation-induced health effects are incidence of cancers and genetic reaction. Equation 3.11 (Munyaradzi et $al.$, 2018 and Taskin et $al.$, 2009) was used to estimate ELCR:

$$ELCR = AEDE \times DL \times RF \qquad (3.11)$$

where, AEDE is the annual effective Dose Equivalent, DL is the average duration of human life (estimated to be 70 years) and RF is risk factor (Sv^{-1}) or fatal cancer risk per sievert. For stochastic effects, which produce low background radiation, the ICRP 60 stipulates a value of 0.29×10^{-3} for public exposure (Munyaradzi et $al.$, 2018 and Taskin et $al.$, 2009).

CHAPTER FOUR

4.0   RESULTS AND DISCUSSION

4.1 Results

The specific activity concentration of NORM in soil collected from Gababiyu artisanal goldmine has been measured using gamma spectrometric technique. The results for the concentration of ^{226}Ra, ^{232}Th and ^{40}K with their respective mean values in Bq.kg^{-1} are shown in Table 4.1. The net counts obtained from gamma spectrometric analysis and specific activities of ^{226}Ra, ^{232}Th and ^{40}K are presented in Appendix A. Specific activity concentrations of ^{226}Ra, ^{232}Th and ^{40}K vary from 10.27±2.88 to 152.60±3.80 Bq.kg^{-1}, 32.67±1.93 to 185.90±6.06 Bq.kg^{-1} and 35.18±1.45 to 947.50±7.51 Bq.kg^{-1} respectively, with mean values of 65.06±4.20, 87.63±2.89 and 267.94±4.29 Bq.kg^{-1}.

The computed radiation hazard indices are shown in Table 4.2. Ra$_{eq}$ varies from 96.67±4.56 to 396.18±13.87 Bq.kg^{-1} with 210.86±8.66 Bq.kg^{-1} mean. Gamma radiation dose 1 m above ground (D) varies from 44.02 to 173.46 nGy.h^{-1} with an average value of 94.16 nGy.h^{-1}. AEDE varies from 0.10 to 0.40 mSv.y^{-1} with mean value of 0.22 mSv.y^{-1}. AGDE varies from 306.24 to 1190.97 µSv.y^{-1} with mean value of 651.47 µSv.y^{-1}. AUI varies from 0.68 to 3.37 with mean of 1.68. H$_{ex}$ varies from 0.26 to 1.07 with mean of 0.57 while the H$_{in}$ varies from 0.32 to 1.40 with mean of 0.75. I$_{\gamma r}$ varies from 0.70 to 2.75 with mean of 1.49. ELCR varies from 0.35×10^{-3} to 1.40×10^{-3} with 0.76×10^{-3} mean value.

Table 4.1: Activity concentrations of NORM in soil samples collected from Gababiyu artisanal goldmine

Sample ID	Activity concentration (Bq/kg)		
	^{226}Ra	^{232}Th	^{40}K
GM01	10.27±2.88	60.12±0.31	183.84±8.58
GM02	129.1±3.40	96.92±3.07	236.02±1.56
GM03	19.18±2.80	48.21±0.94	144.85±5.47
GM04	89.13±6.75	38.06±4.72	137.82±1.14
GM05	41.44±3.08	80.80±0.28	732.34±6.44
GM06	17.50±2.24	78.76±1.53	277.74±7.94
GM07	152.60±3.80	124.72±1.34	166.84±3.00
GM08	81.07±2.84	91.57±2.20	281.65±6.38
GM09	38.48±3.00	66.33±1.34	247.06±6.86
GM10	120.19±4.99	185.90±6.06	135.41±2.90
GM11	61.45±4.68	59.88±2.08	189.57±2.63
GM12	75.64±3.36	96.41±1.42	228.51±2.57
GM13	25.05±0.92	63.62±0.20	233.34±8.85
GM14	84.95±4.52	83.75±1.02	184.69±5.79
GM15	28.33±1.08	32.67±1.93	281.65±9.49
GM16	95.68±8.47	66.80±7.67	174.34±1.24
GM17	89.90±3.32	79.62±0.39	291.20±3.49
GM18	33.52±2.60	60.43±2.01	82.48±3.00
GM19	51.06±3.80	73.41±1.61	232.26±5.68
GM20	41.36±5.43	109.23±1.85	297.96±6.01
GM21	92.40±7.79	110.45±6.88	333.66±1.00
GM22	88.66±3.76	75.77±0.83	260.69±0.97
GM23	41.71±4.00	52.49±1.10	35.18±1.45
GM24	22.22±1.68	68.34±1.42	135.46±6.06
GM25	108.42±4.43	98.45±5.23	157.34±0.72
GM26	41.40±4.44	83.00±2.24	209.90±5.63
GM27	97.32±5.51	92.01±5.62	162.05±1.20
GM28	36.39±3.20	45.85±4.76	153.26±0.47
GM29	102.91±7.95	132.90±8.85	232.20±1.56
GM30	42.03±3.76	100.46±0.24	130.10±6.92
GM31	34.52±2.00	68.10±0.98	168.77±6.76
GM32	13.83±6.63	99.75±0.24	405.86±6.97
GM33	99.79±7.79	122.64±3.26	322.55±1.06
GM34	22.58±0.76	61.18±0.39	829.41±7.83
GM35	116.79±2.88	123.07±2.56	93.90±0.21
GM36	75.60±5.03	137.18±4.95	408.27±7.99
GM37	83.61±7.47	83.08±9.24	91.06±0.39
GM38	49.07±4.24	165.69±6.68	947.50±7.51
GM39	109.58±5.23	87.41±5.15	155.62±1.02
GM40	37.56±5.47	100.30±3.07	745.27±6.97
Min.	10.27±2.88	32.67±1.93	35.18±1.45
Max.	152.60±3.80	185.90±6.06	947.50±7.51
Mean	65.06±4.20	87.63±2.89	267.94±4.29

Table 4.2: Radiation hazard indices of soil samples collected from Gababiyu artisanal goldmine

Sample ID	Ra$_{eq}$ (Bq/Kg)	Radiological dose			Radiation hazard indices (≤1)				ELCR (×10^{-3})
		D (nGy/h)	AEDE (mSv/y)	AGDE (µSv/y)	AUI	H$_{ex}$	H$_{in}$	I$_{\gamma r}$	
GM01	110.29±3.99	48.72	0.11	340.75	0.84	0.30	0.33	0.79	0.39
GM02	285.71±7.90	128.03	0.29	878.16	2.38	0.77	1.12	1.99	1.03
GM03	99.19±4.57	44.02	0.10	306.24	0.77	0.27	0.32	0.71	0.35
GM04	154.10±13.58	69.91	0.16	477.77	1.29	0.42	0.66	1.07	0.56
GM05	213.20±3.96	98.49	0.23	695.74	1.42	0.58	0.69	1.57	0.79
GM06	151.37±5.04	67.24	0.15	470.49	1.14	0.41	0.46	1.09	0.54
GM07	343.60±5.94	152.79	0.35	1045.24	2.93	0.93	1.34	2.38	1.23
GM08	233.56±6.47	104.51	0.24	721.73	1.88	0.63	0.85	1.64	0.84
GM09	152.24±5.43	68.14	0.16	473.74	1.18	0.41	0.52	1.08	0.55
GM10	396.18±13.87	173.46	0.40	1190.97	3.37	1.07	1.40	2.75	1.40
GM11	161.58±7.85	72.47	0.17	499.73	1.31	0.44	0.60	1.13	0.58
GM12	230.94±5.58	102.71	0.24	708.47	1.88	0.62	0.83	1.62	0.83
GM13	133.88±1.88	59.73	0.14	416.60	1.02	0.36	0.43	0.96	0.48
GM14	218.80±6.42	97.53	0.22	670.56	1.81	0.59	0.82	1.53	0.78
GM15	96.67±4.56	44.57	0.10	312.55	0.68	0.26	0.34	0.70	0.36
GM16	204.52±19.52	91.82	0.21	629.62	1.71	0.55	0.81	1.42	0.74
GM17	226.05±4.15	101.77	0.23	702.05	1.82	0.61	0.85	1.59	0.82
GM18	126.20±5.69	55.43	0.13	382.10	1.05	0.34	0.43	0.88	0.45
GM19	173.80±6.54	77.62	0.18	537.57	1.38	0.47	0.61	1.23	0.62
GM20	220.32±8.54	97.50	0.22	677.92	1.73	0.60	0.71	1.57	0.78
GM21	275.85±17.70	123.31	0.28	851.96	2.22	0.75	1.00	1.94	0.99
GM22	216.96±5.01	97.60	0.22	672.54	1.76	0.59	0.83	1.52	0.79
GM23	119.41±5.68	52.44	0.12	359.36	1.02	0.32	0.44	0.83	0.42
GM24	130.26±4.17	57.19	0.13	396.83	1.04	0.35	0.41	0.92	0.46
GM25	261.17±11.96	116.12	0.27	795.97	2.20	0.71	1.00	1.81	0.93
GM26	176.12±8.07	78.01	0.18	540.77	1.40	0.48	0.59	1.25	0.63
GM27	241.22±13.64	107.29	0.25	736.18	2.02	0.65	0.91	1.68	0.86
GM28	113.68±10.03	50.90	0.12	352.22	0.90	0.31	0.41	0.80	0.41
GM29	310.62±20.71	137.50	0.32	946.41	2.58	0.84	1.12	2.17	1.11
GM30	195.56±4.63	85.52	0.20	590.66	1.61	0.53	0.64	1.37	0.69
GM31	144.79±3.92	64.12	0.15	444.33	1.16	0.39	0.48	1.02	0.52
GM32	187.55±7.51	83.56	0.19	587.12	1.37	0.51	0.54	1.36	0.67
GM33	299.80±12.53	133.63	0.31	922.26	2.43	0.81	1.08	2.11	1.08
GM34	173.78±1.92	81.97	0.19	585.93	1.02	0.47	0.53	1.32	0.66
GM35	299.83±6.54	132.21	0.30	904.80	2.57	0.81	1.13	2.07	1.06
GM36	302.98±12.73	134.81	0.31	935.22	2.39	0.82	1.02	2.15	1.08
GM37	209.30±20.70	92.61	0.21	634.23	1.78	0.57	0.79	1.45	0.75
GM38	358.65±14.36	162.26	0.37	1141.72	2.53	0.97	1.10	2.62	1.31
GM39	246.42±12.67	109.91	0.25	752.82	2.08	0.67	0.96	1.71	0.88
GM40	238.18±10.39	109.01	0.25	769.34	1.62	0.64	0.75	1.75	0.88
Min.	96.67±4.56	44.02	0.10	306.24	0.68	0.26	0.32	0.70	0.35
Max.	396.18±13.87	173.46	0.40	1190.97	3.37	1.07	1.40	2.75	1.40
Mean	210.86±8.66	94.16	0.22	651.47	1.68	0.57	0.75	1.49	0.76

4.2 Discussion

4.2.1 Activity concentrations of NORM

The distributions of ^{226}Ra, ^{232}Th and ^{40}K in the soil samples depict variations of radiation levels within the mining area which conforms with results of existing literature.

The activity concentration of ^{226}Ra in the studied soil samples varied with mean value of 65.06 Bq/kg. This value is above the UNSCEAR (2000) global average of 35.00 Bq/kg and indicates significant amount of ^{226}Ra in the soil within the studied area. However, the mean ^{226}Ra concentration of this study is moderate compared to those measured in Guateng Province (780.30 Bq.kg^{-1}) by Kamunda *et al.* (2016). Also indicating significant concentration is the 87.63 Bq/kg mean observed for ^{232}Th in this study that is above the global average of 30.00 Bq/kg. The average ^{232}Th concentration of this study was also moderate compared with those determined by Silver *et al.* (2016) and Doyi *et al.* (2013) in Southwest Uganda (216.00 Bq.kg^{-1}) and Tongo 294.43 Bq.kg^{-1} respectively.

The 267.94 Bq.kg^{-1}average concentration of ^{40}K determined in this study is far below the global average of 400.00 Bq/kg. Thus, indicating minimal deposits of ^{40}K in the mining area. However, the concentration levels are much higher than those determined by Kolo *et al.* (2012). These variations are due to natural sources and the accumulation of mine tailings.

The contrast of the specific activities of NORM from this study and those from similar studies are shown in Table 4.3.

Table 4.3: Activity concentration of NORM from this study and similar studies around the world

Country (Region)	Mean activity (Bq.kg⁻¹)			Reference
	^{226}Ra	^{232}Th	^{40}K	
Nigeria (Minna)	65.06	87.63	267.94	This work
Nigeria (Erena, Niger)	49.43	37.69	564.63	Suleiman *et al.* (2018)
Nigeria (Enugu)	33.20	77.70	100.70	Osimobi *et al.* (2018)
Uganda (Southwest)	55.30	216.00	566.93	Silver *et al.* (2016)
Nigeria (Erinmo, Osun)	21.90	23.4	136.50	Nwankpa *et al.* (2016)
South Africa (Guateng province)	785.30	43.90	427.00	Kamunda *et al.* (2016)
Ghana (Perseus goldmine)	65.10	71.80	1168.30	Faanu *et al.* (2016)
Nigeria (Awwal, Kebbi)	23.85	18.80	425.96	Girigisu *et al.* (2014)
Nigeria (Itagunmobi, Osun)	55.30	26.40	505.10	Ademola *et al.* (2014)
Nigeria (Zamfara)	12.12	60.12	462.51	Innocent *et al.* (2013)
Nigeria (Central Nasarawa)	32.52	56.23	403.96	Ibrahim *et al.* (2013)
Nigeria (Birnin-Gwari, Kaduna)	37.36	62.69	997.52	Nasiru *et al.* (2013)
Ghana (Tongo)	66.29	294.43	1964.29	Doyi *et al.* (2013)
Nigeria (Yankadutse, Kaduna)	2.08	47.23	382.01	Abdulkarim *et al.* (2013)
Nigeria (Minna)	7.80	29.40	229.40	Kolo *et al.* (2012)
World Average	35.00	30.00	400.00	UNSCEAR (2000)

4.2.2 Radiological parameters

Radium equivalent activity (Ra$_{eq}$) has mean of 210.86 Bq.kg⁻¹ which is far below the global upper limit of 370 Bq.kg⁻¹ (Kolo *et al.*, 2012 and UNSCEAR, 2000). Thus, indicates radiological safety.

The average gamma radiation dose (D) a metre from the ground due to NORM accumulation around the mining site is 94.16 nGy.h⁻¹. This value is well above the global average of 57 nG.h⁻¹ (Kolo *et al.*, 2019 and UNSCEAR, 2000). However, this value obtained is lower compared with those obtained by Silver *et al.* (2016), Kamunda *et al.* (2016), Doyi *et al.* (2013).

AEDE has mean of 0.22 mSv.y⁻¹ that is far below the 1 mSv.y⁻¹ threshold recommended for public exposure (ICRP, 2007). This value is also less than those obtained by Sabo *et al.* (2018), Faanu *et al.* (2016), Ibrahim *et al.* (2013) and Qureshi *et al.* (2014). Thus,

indicating minimal risk to exposed miners and habitants of surrounding communities of Gababiyu artisanal goldmine.

The comparison of the radiological parameters of this study and those from similar studies are shown in Table 4.4.

Table 4.4: Radiological parameters of this study compared with other reported values around the world

Country (Region)	Ra_{eq} (Bq/kg)	D (nGy/h)	AEDE (mSv/y)	AGDE (µSv/y)	ELCR $\times 10^{-3}$	Reference
Nigeria (Minna)	210.86	94.16	0.22	651.47	0.76	This work
Nigeria (Erena, Niger)	135.78	69.15	0.09	-	-	Suleiman *et al.* (2018)
Nigeria (Luku, Niger)	-	-	1.70	-	-	Sabo *et al.* (2018)
Nigeria (Enugu)	151.40	67.50	0.08	457.10	0.30	Osimobi *et al.* (2018)
Uganda (Southwest Mines)	-	180.00	0.37	-	1.30	Silver *et al.* (2016)
Nigeria (Erinmo, Osun)	-	30.70	0.04	-	-	Nwankpa *et al.* (2016)
South Africa (Guateng province)	880.90	407.1	0.50	-	-	Kamunda *et al.* (2016)
Ghana (Perseus goldmine)	257.80	80.00	0.91	-	-	Faanu *et al.* (2016)
Nigeria (Nasarawa mines)	-	-	<1.00	580.00	-	Aliyu *et al.* (2015)
Nigeria (Awwal, Kebbi)	-	-	0.04	-	-	Girigisu *et al.* (2014)
Nigeria (Itagunmobi, Osun)	132.14	-	0.08	439.73	-	Ademola *et al.* (2014)
Pakistan (Hunza, Gilgit and Indus Rivers)	190.89	87.47	0.92	-	3.21	Qureshi *et al.* (2014)
Nigeria (Zamfara)	-	59.70	0.07	-	-	Innocent *et al.* (2013)
Nigeria (Central Nasarawa)	141.56	-	5.81	-	-	Ibrahim *et al.* (2013)
Ghana (Tongo)	-	290.00	0.44	-	-	Doyi *et al.* (2013)
Nigeria (HI, Minna)	67.50	31.30	0.04	217.80	-	Kolo *et al.* (2012)
Ghana (Tarkwa goldmine)	-	29.90	0.69	-	-	Faanu *et al.* (2011)
Kenya (Nyanza)	-	42.00	0.05	-	-	Odumo *et al.* (2011)
Nigeria (Minna)	-	-	0.19	-	-	Olarinoye *et al.* (2010)
Ghana (Ashanti)	-	-	0.26 / 1.83*	-	-	Darko *et al.* (2005)
World Average	370.00	57.00	1.00	300.00	0.29	ICRP (2007), UNSCEAR (2000)

*Underground mine

The mean 651.74 $\mu Sv.y^{-1}$ recorded for AGDE in this study is far greater than the 300 $\mu Sv.y^{-1}$ global threshold (Aliyu *et al.*, 2015 and Xinwei *et al.*, 2006). This value is also higher than the 217.80 $\mu Sv.y{-1}$ measured within the Higher Institutions in Minna Metropolis by Kolo *et al.* (2012). Consequently, the AGDE of this study indicates significant dose to the gonads of miners of Gababiyu artisanal gold mine.

The mean AUI for the mining area is 1.68. This satisfies the <2 threshold and corresponds to the AEDE below 1 $mSv.y^{-1}$ (Osimobi *et al.*, 2018 and Sivakumar *et al.*, 2014). Thus, signifies radiological safety.

The average values of 0.75 and 0.57 were recorded for H_{in} and H_{ex} respectively. These are below the unity threshold stipulated by UNSCEAR (2000) and conform with the 0.22 $mSv.y^{-1}$ obtained in this study. Thus, signifies minimal risk to gamma radiation external exposure to air and hazardous effects of radon to the respiratory organs.

I_{yr} has average of 1.49. This value is above the global screening value of unity for building materials (Osimobi *et al.*, 2018 and Sivakumar *et al.*, 2014). Thus, suggests that the soil from Gababiyu artisanal goldmine is not suitable as aggregate for building materials.

ELCR of this study varied with a mean of 0.76×10^{-3} that is 2.6 times the global mean of 0.29×10^{-3} (Taskin *et al.*, 2009 and Munyaradzi *et al*, 2018). However, ELCR of this study is far below the 3.21×10^{-3} realised in the North area of Pakistan by Qureshi *et al.* (2014). Numerous cancer deaths reported in that region were attributed the high radioactivity levels due to NORM (Qureshi *et al.*, 2014). Thus, the ELCR of this study indicates minimal cancer risk to the artisanal gold miners and populace of surrounding communities.

CHAPTER FIVE

5.0 CONCLUSION AND RECOMMENDATIONS

5.1 Conclusion

Human activities incite radiological contamination of the environment which results to significant human health challenges. Forty soil samples were collected around Gababiyu artisanal goldmine in Minna, Nigeria to assess the radiological implications of gold mining in the area. The soil samples were cleared of debris, placed into well labeled polyethylene bags and conveyed to the laboratory for preparation and analysis using gamma spectrometric technique.

Specific activities of ^{226}Ra, ^{232}Th and ^{40}K in sequence vary from 10.27 ± 2.88 to 152.60 ± 3.80 Bq.kg^{-1}, 32.67 ± 1.93 to 185.90 ± 6.06 Bq.kg^{-1} and 35.18 ± 1.45 to 947.50 ± 7.51 Bq.kg^{-1} respectively. Ra$_{eq}$ varies from 96.67 ± 4.56 to 396.18 ± 13.87 Bq.kg^{-1} with 210.86 ± 8.66 Bq.kg^{-1} mean. The average specific activity values for ^{226}Ra, ^{232}Th and ^{40}K were 65.06, 87.63 and 267.94 Bq/kg in sequence. These values except for ^{40}K were above the UNSCEAR global mean values of 35.00 Bq/kg for ^{226}Ra, 30.00 Bq/kg for ^{232}Th and 400.00 Bq/kg for ^{40}K. Although, the specific activities of ^{226}Ra, ^{232}Th and ^{40}K give an indication of their soil contamination, no immediate radiological danger is envisaged. However, the Annual Gonadal Dose Equivalent of 651.74 µSv.y^{-1} obtained in this study was above the global screening level of 300.00 µSv.y^{-1}. Therefore, indicates potential risk to the reproductive organs of the miners. The gamma representative index of Gababiyu artisanal goldmine reveals that the soil is not suitable as aggregate for building material. Other computed radiological hazard parameters for the soil samples analysed were all within

safety limits for public exposure. Thus, the radiological impact of artisanal mining of gold in the Gababiyu bears minimal significance.

5.2 Recommendations

Artisanal miners are unaware of the environmental and health implications of mining activities. Concentration levels or NORM above global average were realised for Gababiyu artisanal gold mine in Minna Metropolis. Thus, there is need for further investigations described as follows:

1. Plants and food crops grown within the mining sites should be assessed for NORM concentrations to determine soil-plant transfer ratio. This will aid in assessing the dose of radiation ingested by people who consume the cultivated crops.

2. Tailings carried over by streams to neighbouring communities should be assessed for radiological contents. This should be done for both the tailings and water to ascertain the quality of the water consumed in the affected communities.

3. The Nigerian Nuclear Regulatory Authority (NNRA) should impose radiological guidelines and regulations in artisanal mining areas to protect the miners and the environment at large from high radiation exposure.

REFERENCES

Abdulkarim, M. S., & Umar, S. (2013). An investigation of natural radioactivity around gold mining sites in Birnin Gwari North Western Nigeria. *Research Journal of Physical Sciences*, *1*(7), 20–23.

Abdulkarim, M. S., Zakari, I. Y., & Sadiq, U. (2013). Assessment of activity concentration of the naturally occurring radioactive materials (NORM) in the Yankandutse artisanal gold mining belt of Kaduna, Nigeria. *IOSR Journal of Applied Physics (IOSR-JAP)*, *4*(3), 58–61.

Ademola, A. K., Bello, A. K., & Adejumobi, A. C. (2014). Determination of natural radioactivity and hazard in soil samples in and around gold mining area in Itagunmodi, south-western, Nigeria. *Journal of Radiation Research and Applied Sciences*, *7*(3), 249–255. https://doi.org/10.1016/j.jrras.2014.06.001

AGI. (2019). What are the main methods of mining? Retrieved from American Geoscience Institute website: https://www.americangeosciences.org/critical-issues/faq/what-are-main-mining-methods

Ahmed, S. N. (2007). *Physics and Engineering of Radiation Detection* (6th Ed.). Amsterdam: Academic Press.

Ajibade, A. C. (1976). Provisional classification and correlation of the schist belt in Northwestern Nigeria. *Elizabethan Publishing Co, Ibadan*, 85–87.

Ako, T. A., Onoduku, U. S., Oke, S. A., Adamu, I. A., Ali, S. E., Mamodu, A., & Ibrahim, A. T. (2014). Environmental impact of artisanal gold mining in Luku, Minna, Niger State, North Central Nigeria. *Journal of Geosciences and Geomatics*, *2*(1), 28–37. https://doi.org/10.12691/jgg-2-1-5

Al-Gazaly, H. H., Al-Ulim, Mahdi, A. B., Al-Hamidawi, A. A., & Al-Abbasi, A. M. (2014). Natural radioactivity in soil at regions around the uranium mine in. *Advances in Applied Science Research*, *5*(1), 13–17.

Alharbi, S. H. (2016). Measurement and Monitoring of Naturally Occurring Radioactive Materials for Regulation. Retrieved from Queensland University of Technology website: https://eprints.qut.edu.au/98122/1/Sami_Alharbi_Thesis.pdf

Aliyu, A. S., Ibrahim, U., Akpa, C. T., Garba, N. N., & Ramli, A. T. (2015). Health and ecological hazards due to natural radioactivity in soil from mining areas of Nasarawa State, Nigeria. *Isotopes in Environmental and Health Studies*, *51*(3), 448–468. https://doi.org/10.1080/10256016.2015.1026339

Alpen, E. L. (1998). *Radiation Biophysics* (2nd Ed.). San Diego: Academic Press.

Ashraf, E. M. K., Layia, H. A., Amany, A. A., & Al-Omran, A. M. (2010). NORM in clay deposits. *Proceedings of Third European IRPA Congress, Helsinki, Finland,* 1–9.

Bailey, D. L., Humm, J. L., Todd-Pokropek, A., & Aswegen, A. V. (2014). *Nuclear Medicine Physics: A Handbook for Students and Teachers*. Vienna: IAEA.

Berekta, J., & Mathew, P. J. (1985). Natural radioactivity in Australian building materials, industrial waste and by- product. *Health Physics*, *48*, 87–95.

Bertulani, C. A. (2007). *Nuclear Physics in a Nutshell*. New Jersey: Princeton University Press.

Bewick, S., Parsons, R., Forsythe, T., Robinson, S., & Dupon, J. (2019). Types of Radioactivity: Alpha, Beta, and Gamma Decay. Retrieved August 22, 2019, from https://chem.libretexts.org/Bookshelves/Introductory_Chemistry/Map%3A_Introducto ry_Chemistry_(Tro)/17%3A_Radioactivity_and_Nuclear_Chemistry/17.03%3A_Type s_of_Radioactivity%3A_Alpha%2C_Beta%2C_and_Gamma_Decay

Candeias, C., Ávlla, P., Coelho, P., & Teixeira, J. P. (2018). Mining Activities: Health Impacts. In *Encyclopedia of Environmental Health, 2nd Edition* (pp. 1–21). Elsevier Inc. https://doi.org/10.1016/B978-0-12-409548-9.11056-5

Chandrasekaran, A., Ravisankar, R., Senthilkumar, G., Thillaivelavan, K., Dhinakaran, B., Vijayagopal, P., … Venkatraman, B. (2014). Spatial distribution and lifetime cancer risk due to gamma radioactivity in Yelagiri Hills, Tamilnadu, India. *Egyptian Journal of Basic and Applied Sciences*, *1*(1), 38–48.

Cherry, S. R., Sorenson, J. A., & Phelps, M. E. (2012). *Physics in Nuclear Medicine* (4th ed.). Philadelphia: Elsevier Saunders.

Darko, E. O., Tetteh, G. K., & Akaho, E. H. K. (2005). Occupational radiation exposure to NORM in a gold mine. *Radiation Protection Dosimetry*, *114*(4), 538–545. https://doi.org/10.1093/rpd/nci300

Doyi, I., Oppon, O. C., Glover, E. T., Gbeddy, G., & Kokroko, W. (2013). Assessment of occupational radiation exposure in underground artisanal gold mines in Tongo, upper East region of Ghana. *Journal of Environmental Radioactivity*, *126*, 77–82. https://doi.org/10.1016/j.jenvrad.2013.07.007

Faanu, A., Adukpo, O. K., Tettey-Larbi, L., Lawluvi, H., Kpeglo, D. O., Darko, E. O., … Agyeman, L. (2016). Natural radioactivity levels in soils, rocks and water at a mining concession of Perseus gold mine and surrounding towns in Central Region of Ghana. *SpringerPlus*, *5*(1), 1–16. https://doi.org/10.1186/s40064-016-1716-5

Faanu, A., Adukpo, O. K.., Kansaana, C., Tettey-Larbi, L., Lawluvi, H., Kpeglo, D. O., … Agyeman, L. (2016). Impact assessment of naturally occurring radioactive materials on the public from gold mining and processing at Newmont Golden Ridge Limited, Akyem, Eastern Region of Ghana. *Radiation Protection and Environment*, *39*(3), 155–164. https://doi.org/10.4103/0972-0464.194962

Faanu, A., Ephraim, J. H., & Darko, E. O. (2011). Assessment of public exposure to naturally occurring radioactive materials from mining and mineral processing activities of Tarkwa Goldmine in Ghana. *Environmental Monitoring Assessment*, (180), 15–29. https://doi.org/10.1007/s10661-010-1769-9

Ghoshal, S. N. (2014). *Nuclear Physics* (Revised). New Delhi: S. Chand.

Girigisu, S., Ibeanu, I. G. E., Adeyemo, D. J., Onoja, R. A., Bappah, I. A., & Okoh, S.

(2014). Assessment of radiological levels in soils from artisanal gold mining exercises at Awwal, Kebbi State, Nigeria. *Research Journal of Applied Sciences, Engineering and Technology*, *7*(14), 2899–2904. https://doi.org/10.19026/rjaset.7.618

Haribala, Hu, B., Wang, C., Gerilemandahu, Xu, X., Zhang, S., … Li, Y. (2016). Assessment of radioactive materials and heavy metals in the surface soil around uranium mining area of Tongliao, China. *Ecotoxicology and Environmental Safety*, *130*, 185–192. https://doi.org/10.1016/j.ecoenv.2016.04.002

Hilson, G. (2002). The environmental impact of small-scale gold mining in Ghana: Identifying problems and possible solutions. *Geographical Journal*, *168*(1), 57–72. https://doi.org/10.1111/1475-4959.00038

Hollaway, J. (1993). Review of technology for the successful development of small scall mining. *Chamber of Mines Journal*, *35*, 19–25.

IAEA. (2003). *Guidelines for radioelement mapping using gamma ray spectrometry data (IAEA-TECDOC-1363)*. Vienna: International Atomic Energy Agency.

Ibraheem, A. A., El-Taher, A., & Alruwaili, M. H. M. (2018). Assessment of natural radioactivity levels and radiation hazard indices for soil samples from Abha, Saudi Arabia. *Results in Physics*, *11*, 325–330. https://doi.org/10.1016/j.rinp.2018.09.013

Ibrahim, U., Akpa, T. C., & Daniel, I. H. (2013). Assessment of radioactivity concentration in soil of some mining areas in Central Nasarawa State, Nigeria. *Science World Journal*, *8*(2), 7–12.

ICRP. (2007). The 2007 Recommendations of the International Commission on Radiological Protection ICRP. *ICRP Publication 103*, *37*(2–4).

Innocent, A. J., Onimisi, M. Y., & Jonah, S. A. (2013). Evaluation of naturally occurring radionuclide materials in soil samples collected from some mining sites in Zamfara State, Nigeria. *British Journal of Applied Science & Technology*, *3*(4), 684–692.

Jain, R. K., Cui, Z., & Domen, J. K. (2016). Environmental Impacts of Mining. In *Environmental Impact of Mining and Mineral Processing; Management, Monitoring, and Auditing Strategies* (pp. 53–157). Amsterdam: Elsevier. https://doi.org/10.1016/B978-0-12-804040-9.00004-8

Jibiri, N., Isinkaye, M., & Momoh, H. (2014). Assessment of radiation exposure levels at Alaba e-waste dumpsite in comparison with municipal waste dumpsites in southwest Nigeria. *Journal of Radiation Research and Applied Sciences*, *7*(4), 536–541.

Kakani, S. L., & Kakani, S. (2008). *Nuclear and Particle Physics*. New Delhi: Viva Books.

Kamunda, C., Mathuthu, M., & Madhuku, M. (2016). An assessment of radiological hazards from gold mine tailings in the province of Gauteng in South Africa. *International Journal of Environmental Research and Public Health*, *13*(1). https://doi.org/10.3390/ijerph13010138

Khan, F. M. (2003). *The Physics of Radiation Therapy* (3rd ed.). Philadelphia: Lippincott Williams & Wilkins.

Kolo, M. T., Aziz, S. A. A., Khandaker, M. U., Asaduzzaman, K., & Amin, Y. M. (2015). Evaluation of radiological risks due to natural radioactivity around Lynas advanced material plant environment, Kuantan, Pahang, Malaysia. *Environmental Science and Pollution Research*, *22*(17), 13127–13136. https://doi.org/10.1007/s11356-015-4577-5

Kolo, M. T., Baba-Kutigi, A. N., Olarinoye, I. O., & Sharifat, I. (2012). Assessment of natural radioactivity levels and radiation hazards in the tertiary institutions in Minna, Niger State, Nigeria. *Continental Journal of Environmental Sciences*, *6*(3), 25–31. https://doi.org/10.5707/cjenvsci.2012.6.3.25.31

Kolo, M. T., Khandaker, M. U., & Shuaibu, H. K. (2019). Natural radioactivity in soils around mega coal-fired cement factory in Nigeria and its implications on human health and environment. *Arabian Journal of Geosciences*, *12*(15). https://doi.org/10.1007/s12517-019-4607-6

Kuan, L. S., Wagiran, H., & Ramli, A. T. (2009). Measurement of natural radioactivity in soil samples from hotspot areas around Kampung Sungai Durian, Kinta District, Perak. *Prosiding Seminar Kebangsaan Teknologi Makmal*, *9*, 7–10.

Lacerda, L. D., & Salomons, W. (1998). *Mercury from gold and silver mining: a chemical timebomb?* New York: Springer.

Mathuthu, M., Kamunda, C., & Madhuku, M. (2016). Modelling of radiological health risks from gold mine tailings in wonderfonteinspruit catchment area, South Africa. *International Journal of Environmental Research and Public Health*, *13*(6), 570-581. https://doi.org/10.3390/ijerph13060570

Meech, J. A., Veiga, M. M., & Tromans, D. (1993). Reactivity of mercury from gold mining activities in darkwater ecosystems. *Ambio*, *102*, A59–A67.

Mireku-Gyimah, D., & Suglo, R. S. (1993). The state of gold mining in Ghana. *Transactions of the Institute of Mining and Metallurgy*, *102*, A59–A57.

Morsy, Z., El-Wahab, M. A., & El-Faramawy, N. (2012). Determination of natural radioactive elements in Abo Zaabal, Egypt by means of gamma spectroscopy. *Annals of Nuclear Energy*, *44*, 8–11.

Munyaradzi, Z., Anna, K. N., & Makondelele, T. V. (2018). Excess lifetime cancer risk due to natural radioactivity in soils: Case of Karibib town in Namibia. *African Review of Physics*, *13*, 71–78.

Mustoe-Playfair, H. (2011). Scintillator counter as a spectrometer. Retrieved from https://commons.m.wikimedia.org/wiki/File:Scintillation_counter_as_a_spectrometer.jpg#mw-jump-to-license

Nasiru, R., Zakari, I. Y., & Abdullahi, M. A. (2013). Distribution of gamma emitting radionuclides in gold ore mine from Birnin Gwari artisanal goldmine Kaduna State Nigeria. *Research Journal of Applied Sciences, Engineering and Technology*, *6*(17), 3255–3258. https://doi.org/10.19026/rjaset.6.3631

Njinga, R. L., Jonah, S. A., & Gomina, M. (2015). Preliminary investigation of naturally

occurring radionuclides in some traditional medicinal plants used in Nigeria. *Journal of Radiation Research and Applied Sciences*, *8*, 208–215. https://doi.org/10.1016/j.jrras.2015.01.001

Nwankpa, A. C., Agwu, K. K., & Ikusika, A. (2016). Baseline radiation in gold mining area in Erinmo Osun State, Nigeria. *International Journal of Advances in Scientific Research and Engineering*, *2*(1), 1–7.

NYSDH. (2007). Radiation and Health. Retrieved from New York State Department of Health website: https://www.health.ny.gov/publications/4402.pdf

Odumo, O. B., Mustapha, A. O., Patel, J. P., & Angeyo, H. K. (2011). Radiological survey and assessment of associated activity concentration of the naturally occurring radioactive materials (NORM) in the Migori artisanal gold mining belt of southern Nyanza, Kenya. *Applied Radiation and Isotopes*, *69*(6), 912–916. https://doi.org/10.1016/j.apradiso.2011.02.016

Okere, R. (2018, July 25). Nigeria's thriving illegal gold mining activities and challenge of lead poisoning. *Energy-TheGuardian Nigerian News*. Retrieved from https://guardian.ng/energy/nigerias-thriving-illegal-gold-mining-activities-and-challenge-of-lead-poisoning/

Olarinoye, I. O., Ibrahim, S., Baba-Kutigi, A. N., Kolo, M. T., & Aladeniyi, K. (2010). Measurement of background gamma radiation levels at two tertiary institutions in Minna, Nigeria. *Journal of Applied Sciences and Environmental Management*, *14*(1), 59–62. https://doi.org/10.4314/jasem.v14i1.56491

Osimobi, J. C., Avwiri, G. O., & Agbalagba, E. O. (2018). Radiometric and radiogenic heat evaluation of natural radioactivity in soil around solid minerals mining environment in South-Eastern Nigeria. *Environmental Processes*, *5*(4), 859–877. https://doi.org/10.1007/s40710-018-0336-1

Pure Earth. (2008). Artisanal Gold Mining. Retrieved from Pure Earth website: https://www.worstpolluted.org/projects_reports/display/56

Qureshi, A. A., Tariq, S., Din, K. U., Manzoor, S., Calligaris, C., & Waheed, A. (2014). Evaluation of excessive lifetime cancer risk due to natural radioactivity in the rivers sediments of Northern Pakistan. *Journal of Radiation Research and Applied Sciences*, *7*(4), 438–447. https://doi.org/10.1016/j.jrras.2014.07.008

Raghavendra, T., Vishwaprasad, K., Kalyani, G., Vijayalakshmi, T., Himabindu, V., Arunachalam, J., … Tripathi, R. M. (2019). Assessment of natural radioactivity in soils around the proposed uranium mining site of Lambapur – Peddagattu and Seripally, India. *Journal of the Geological Society of India*, *93*(2), 223–227. https://doi.org/10.1007/s12594-019-1156-2

Raja, P. M. V., & Barron, A. R. (2009). Principles of Gamma-ray Spectroscopy and Applications in Nuclear Forensics - Physical Methods in Chemistry and Nano Science - OpenStax CNX. https://doi.org/ba27839d-5042-4a40-afcf-c0e6e39fb454@25.2

Reddy, V. K. K., Reddy, G. C., Sagar, V. D., Reddy, Y. P., & Reddy, R. K. (2012).

Environmental radioactivity studies in the proposed Lambapur and Peddagattu uranium mining areas of Andhra Pradesh, India. *Radiation Protection Dosimetry*, *151*(2), 290–298. https://doi.org/10.1093/rpd/ncs005

Sabo, A., Sadiq, L. S., & Gamba, J. (2018). radiological assessment of artisanal gold mining sites in Luku, Niger State, Nigeria. *Journal of Environment Pollution and Human Health*, *6*(2), 45–50. https://doi.org/10.12691/jephh-6-2-1

Saïdou, T. S., Hosoda, M., Joseph, E. N. N., Akata, N., Flore, T. S. Y., … Didier, T. S. S. (2019). Natural radiation exposure to the public in mining and ore bearing regions of Cameroon. *Radiation Protection Dosimetry*, 1–6. https://doi.org/10.1093/rpd/ncz176

Silver, T. E. R., Edward, J., Richard, O., Mugaiga, A., & Ben, E. D. D. (2016). Determination of natural radioactivity levels due to mine tailings from selected mines in Southwestern Uganda. *Journal of Environment and Earth Science*, *6*(6), 154–163.

Sivakumar, S., Chandrasekaranb, A., Ravisankarc, R., Ravikumarc, S., Prince, M. J., Prakash, J., … Jose, M. T. (2014). Measurement of natural radioactivity and evaluation of radiation hazards in coastal sediments of east coast of Tamilnadu using statistical approach. *Journal of Taibah University for Science*, *8*, 375–384.

Stranden, E. (1976). Some aspects on radioactivity of building materials. *Physical Norvegica*, *8*, 167–177.

Suleiman, I. K., Agu, M. N., & Onimisi, M. Y. (2018). Evaluation of naturally occurring radionuclide in soil samples from Erena mining sites in Niger State, Nigeria. *Current Journal of Applied Science and Technology*, *27*(6), 1–12. https://doi.org/10.9734/cjast/2018/41562

Taskin, H., Karavus, M., Ay, P., Topuzoglu, A., Hidiroglu, S., & Karahan, G. (2009). Radionuclide concentrations in soil and lifetime cancer risk due to gamma radioactivity in Kirklareli, Turkey. *Journal of Environmental Radioactivity*, *100*(1), 49–53. https://doi.org/10.1016/j.jenvrad.2008.10.012

Turner, J. E. (2007). *Atoms, Radiation, and Radiation Protection* (3rd ed.). Weinheim: Wiley-VCH Verlag GmbH. https://doi.org/10.1002/9783527616978

UNEP. (2016). Radiation: Effects and Sources. Retrieved March 12, 2019, from http://wedocs.unep.org/handle/20.500.11822/7790

UNSCEAR. (2000). *Sources and Effects of Ionizing Radiation. Report of the United Nations Scientific Committee on the Effects of Atomic Radiation to the General Assembly*. United Nations, New York.

USNRC. (2017). Natural and Man-Made Radiation Sources. Retrieved September 3, 2019, from https://www.nrc.gov/reading-rm/basic-ref/students/for-educators/06.pdf

Varier, M. K. (2009). *Nuclear radiation detection: Measurements and analysis*. New Delhi, India: Narosa Publishing House.

WNA (2014). Naturally-Occurring Radioactive Materials (NORM). Retrieved from World

Nuclear Association website: http://www.world-nuclear.org/info/Safety-and-Security/Radiation-and-Health/Naturally-Occurring-Radioactive-Materials-NORM/

Xinwei, L., Lingqing, W., Xiaodan, J., Leipeng, Y., & Gelian, D. (2006). Specific activity and hazards of Archeozoic-Cambrian rock samples collected from the Weibei area of Shaanxi, China. *Radiation Protection Dosimetry*, *118*(3), 352–359.